Triple critical point and emerging temperature scales in $SU(N)$ ferromagnetism at large N

Alexios P. Polychronakos[1,2] and **Konstantinos Sfetsos**[3]

[1] Physics Department, the City College of New York
160 Convent Avenue, New York, NY 10031, USA
apolychronakos@ccny.cuny.edu

[2] The Graduate School and University Center, City University of New York
365 Fifth Avenue, New York, NY 10016, USA
apolychronakos@gc.cuny.edu

[3] Department of Nuclear and Particle Physics,
Faculty of Physics, National and Kapodistrian University of Athens,
Athens 15784, Greece
ksfetsos@phys.uoa.gr

Abstract

The non-Abelian ferromagnet recently introduced by the authors, consisting of atoms in the fundamental representation of $SU(N)$, is studied in the limit where N becomes large and scales as the square root of the number of atoms n. This model exhibits additional phases, as well as two different temperature scales related by a factor $N/\ln N$. The paramagnetic phase splits into a "dense" and a "dilute" phase, separated by a third-order transition and leading to a triple critical point in the scale parameter n/N^2 and the temperature, while the ferromagnetic phase exhibits additional structure, and a new paramagnetic-ferromagnetic metastable phase appears at the larger temperature scale. These phases can coexist, becoming stable or metastable as temperature varies. A generalized model in which the number of $SU(N)$-equivalent states enters the partition function with a nontrivial weight, relevant, e.g., when there is gauge invariance in the system, is also studied and shown to manifest similar phases, the dense-dilute phase transition becoming second-order in the fully gauge invariant case.

Contents

1 Introduction

Magnetic systems with higher internal $SU(N)$ symmetry are enjoying a revival in physics. Such systems have been considered in the context of ultracold atoms [1–6] or of interacting atoms on lattice cites [7–13], and were also studied in the presence of $SU(N)$ magnetic fields [14–16].

We have recently constructed a model for ferromagnets with $SU(N)$ degrees of freedom which manifests an intricate and nontrivial phase structure [17]. At zero

1

magnetic field the system has three critical temperatures (vs. only one for $SU(2)$), with a crossover between metastable states. Spontaneous breaking of the global $SU(N)$ symmetry arises in the $SU(N) \rightarrow SU(N-1) \times U(1)$ channel at zero external magnetic field and generalizes to other channels in the presence of non-Abelian magnetic fields. Further, due to the presence of metastable states, the $SU(N)$ system exhibits hysteresis phenomena both in the magnetic field and in the temperature.

This raises the obvious question of whether a modification of the model and/or a different dynamical regime of the model manifest novel features and phases, and this is the topic of the present work. The modification we will consider involves weighing the partition function by a general power of the number of states of each irreducible component of the global $SU(N)$ symmetry, thus modifying the entropy of each such component (the original model corresponds to the power being 1). The new dynamical regime we will consider is the one where the rank of the group N grows large. Nontrivial modifications arise when the scaling is $N \sim \sqrt{n}$, with n the number of atoms in the magnet (playing the role of the volume of the system at the thermodynamic limit), generalizing and putting in a more physical context the infinite-temperature case studied in [18]. The square root scaling implies that modestly large N (much smaller than n) will give rise to new effects.

As we shall demonstrate, the above modified ferromagnet (for zero external magnetic field) develops new phases, splitting the paramagnetic phase of the finite-N ferromagnet into a "dilute" (more paramagnetic) and a "dense" (less paramagnetic) phase, separated from each other by a third-order phase transition and from the ferromagnetic phase by a zeroth-order transition (the free energy is discontinuous) and leading to a triple critical point in the plane of the scale parameter N^2/n and the temperature. Further, an additional high temperature scale emerges, related to the lower one by a factor of order $N/\ln N$, in which the ferromagnetic phase acquires additional structure and a new "mixed" paramagnetic-ferromagnetic phase appears. These phases can coexist over a range of parameters, the ferromagnetic one dominating thermodynamically at lower temperatures, becoming metastable, and eventually disappearing at significantly larger temperatures, while the mixed phase remains metastable at all temperatures. These features persist for all weighting factors for $SU(N)$-equivalent states, with the notable difference that the dense-dilute transition becomes second-order in the "gauge invariant" limit in which the number of states of each irreducible component drops from the partition function (its power becomes zero).

The organization of the paper is as follows: In section 2 we present the essential features of the model and summarize the group theory tools needed for its analysis [19, 17]. In section 3 we analyze the dilute (most paramagnetic) phase and derive its critical transition temperatures; in section 4 we perform the analysis of the dense (less paramagnetic) phase and derive its critical temperatures; and in section 5 we analyze the ferromagnetic phase. In section 6 we study two special cases of the weighting power for the states, the regular one fully taking into account all states, as in standard ferromagnets, and the one with full gauge invariance between states in the same irreducible component, and derive analytical expressions for their transition temperatures. In section 7 we perform the thermodynamic analysis of the various phases, identify the emerging high temperature scale, uncover the "mixed" metastable paramagnetic-ferromagnetic phase, and determine the order of phase transition between the various phases. Finally, in section 8 we present our conclusions.

2   The general model

We consider a set of n atoms, each carrying the fundamental representation of $SU(N)$ and interacting with ferromagnetic-type interactions. Denoting by $j_{r,a}$ the $N \times N$-dimensional generators of $SU(N)$ in the fundamental representation acting on atom r at position $\vec{r}$, the interaction Hamiltonian of the full system is

$$H = \sum_{r,s=1}^{n} c_{\vec{r},\vec{s}} \sum_{a=1}^{N^2-1} j_{r,a} j_{s,a} \, , \tag{2.1}$$

where $c_{\vec{r},\vec{s}} = c_{\vec{r},\vec{s}}$ is the strength of the interaction between atoms r and s. This Hamiltonian involves an isotropic quadratic coupling between the fundamental generators of the n commuting $SU(N)$ groups of the atoms. Assuming translation invariance $c_{\vec{r},\vec{s}} = c_{\vec{r}-\vec{s}}$, and also that the mean-field approximation is valid,[1] each atom will interact with the average of the $SU(N)$ generators of the remaining atoms; that is,

$$\sum_{\vec{r},\vec{s}} c_{\vec{r}-\vec{s}} \, j_{\vec{r},a} \, j_{\vec{s},a} = \sum_{\vec{r}} j_{\vec{r},a} \sum_{\vec{s}} c_{\vec{s}} \, j_{\vec{r}+\vec{s},a} \simeq \sum_{r} j_{r,a} \left(\sum_{\vec{s}} c_{\vec{s}} \right) \frac{1}{n} \sum_{s'=1}^{n} j_{s',a} = -\frac{c}{n} J_a J_a \, , \tag{2.2}$$

---

[1]The validity of the mean field approximation is strongest in three dimensions, since every atom has a higher number of near neighbors and the statistical fluctuations of their averaged coupling are weaker, but is expected to also hold in lower dimensions.

where we defined the total $SU(N)$ generator

$$J_a = \sum_{s=1}^{n} j_{s,a} \qquad (2.3)$$

and the effective mean coupling

$$c = -\sum_{\vec{s}} c_{\vec{s}} . \qquad (2.4)$$

The minus sign is introduced such that ferromagnetic interactions, driving atom states to align, correspond to positive c. Altogether, the effective interaction is proportional to the quadratic Casimir of the total $S(N)$ generators

$$H = -\frac{c}{n} \sum_{a=1}^{N^2-1} J_a^2 . \qquad (2.5)$$

Calculating the partition function involves decomposing the full Hilbert space of the tensor product of n fundamentals of $SU(N)$ into irreducible representations (irreps), each of which has a fixed quadratic Casimir. This is most conveniently done in the fermion momentum representation. Specifically, to each irrep with Young tableau row lengths $\ell_1 \geqslant \ell_2 \geqslant \cdots \geqslant \ell_{N-1}$ we map a set of N distinct non-negative integers $k_1 > k_2 > \cdots > k_N$ such that

$$k_i - k_N = \ell_i + N - i , \qquad \sum_{i=1}^{N} k_i = n + \frac{N(N-1)}{2} . \qquad (2.6)$$

If $n < N, k_N = 0$, but for $n \geqslant N$ all k_i may become nonzero. We label each irrep with its corresponding vector $\mathbf{k} = \{k_1, \ldots, k_N\}$. The relevant quantities for our ferromagnetic model are:

• The dimension (number of states) $\dim(\mathbf{k})$ of the irrep labelled by $\mathbf{k}$, given by

$$\dim(\mathbf{k}) = \frac{\Delta(\mathbf{k})}{\prod_{s=1}^{N-1} s!} , \quad \text{with} \quad \Delta(\mathbf{k}) = \prod_{j>i=1}^{N} (k_i - k_j) . \qquad (2.7)$$

• The quadratic Casimir $C_2(\mathbf{k})$ of irrep $\mathbf{k}$, given by

$$C_2(\mathbf{k}) = \frac{1}{2} \sum_{i=1}^{N} k_i^2 - \frac{1}{2} \left(\frac{n}{N} + \frac{N-1}{2} \right)^2 - \frac{N(N^2-1)}{24} . \qquad (2.8)$$

• The multiplicity $d(n;\mathbf{k})$ of the irrep $\mathbf{k}$ in the decomposition of n fundamentals, given by [19]

$$d(n;\mathbf{k}) = \frac{n!\,\Delta(\mathbf{k})}{\displaystyle\prod_{i=1}^{N} k_i!}\,.\tag{2.9}$$

With the help of the above, the partition function of the model in temperature $T = \beta^{-1}$, consisting of the sum of the Boltzmann factors $e^{-\beta H}$ with H as is (2.5) over all N^n states, can be written as an explicit sum over k_i.

In what follows, we will consider a more general model in which each Boltzmann factor is weighted by a *power* of the number of states $\dim(\mathbf{k})$ in each irrep. Omitting the irrelevant additive constants in the Casimir (2.8), our generalized partition function is given by

$$Z_{w,n} = \sum_{\mathbf{k}} m(w,n;\mathbf{k}) \exp\!\left(\tfrac{\beta c}{2n}\textstyle\sum_{i=1}^{N} k_i^2\right), \quad \sum_{i=1}^{N} k_i = n + \frac{N(N-1)}{2}\,,\tag{2.10}$$

where $m(w,n;\mathbf{k})$ is the generalized thermodynamic multiplicity[2]

$$m(w,n;\mathbf{k}) = \dim(\mathbf{k})^{w-1} d(n;\mathbf{k}) = \frac{n!\,\Delta(\mathbf{k})^{w}}{\left(\displaystyle\prod_{s=1}^{N-1} s!\right)^{w-1}\displaystyle\prod_{i=1}^{N} k_i!}\,.\tag{2.11}$$

The parameter w assigns an exponential weight to the number of states of each irrep, $w = 2$ corresponding to the standard thermodynamic ensemble. Other values of w are relevant in specific contexts. In particular, $w = 1$ would correspond to a situation where $SU(N)$ is a gauge group, and all states transforming in the same irrep are gauge-equivalent and count as a single state. The case $w < 1$ is rather unphysical, since in that case the thermodynamic contribution of an irrep would *diminish* with its number of states. In what follows we are mostly interested in the cases $w = 1$ and $w = 2$, but we keep the discussion general.

As explained in the introduction, when N^2 and n are comparable, the phase structure of the model changes compared to the standard thermodynamic limit $N^2 \ll n$, $w = 2$. What happens in general is that the unbroken (paramagnetic) phase of the

---

[2]This factor was introduced in [18] where the infinite temperature limit of our model was studied and shown to have a rich structure depending on the value of w. A possible additional power in the multiplicity $d(n;\mathbf{k})$ can be absorbed into a redefinition of the remaining parameters of the model in the thermodynamic limit.

standard ferromagnet maps to a phase with a distribution of irreps parametrized by a continuous density of the k_i, while the broken (ferromagnetic) phase corresponds to a continuous distribution plus one isolated k_i, which turns out to be the largest one k_1. We call the first one "lumped" and the second one "disjoint" phases. The lumped (continuous) distribution can either saturate the density limit of 1 for a range of values of k (corresponding to a set of adjacent k_i), or never saturate it. We call the first one "dense" and the second one "dilute" phases. At high temperatures, the disjoint distribution can either correspond to a single-row symmetric irrep, or also have a lumped part corresponding to nonzero lower Young tableau rows. We call the first one simply disjoint, or symmetric, and the second one "lumped-disjoint", or "mixed" phases. Overall, we have three possible phases at lower temperatures (the dilute, the dense, and the disjoint phases) and four possible phases at very high temperatures (the dilute, the dense, the disjoint, and the lumped-disjoint phases), which can coexist. Later in the paper we will analyze the various phases and derive their thermodynamic transitions.

3   Lumped dilute distributions

In the large-n, N limit it is possible and convenient to describe the set of vectors $\mathbf{k}$ in terms of the density $\rho(k)$ of the k_i on the real positive axis. Writing the summand in (2.11) as $e^{-\beta F_{w,n}}$, with F representing the free energy of configuration $\mathbf{k}$, and using the Stirling formula for factorials, we have (for details on passing to the continuum we refer the reader to [18])

$$
\begin{aligned}
\beta F_{w,n}[\rho(k)] = &-\frac{w}{2} \int_0^\infty dk \int_0^\infty dk'\, \rho(k)\rho(k') \ln|k - k'| \\
&+ \int_0^\infty dk\, \rho(k)\left(k(\ln k - 1) - \frac{\beta c}{2n}k^2\right) + (w-1)\sum_{s=1}^{N-1} \ln s! - \ln n!\,,
\end{aligned}
\tag{3.1}
$$

where the last two terms are constant and will be omitted in the subsequent analysis. We will consider distributions $\rho(k)$ that are everywhere differentiable, except at points where $\rho(k)$ becomes 0 or 1.

In the thermodynamic limit $n \gg 1$, the sum (integral) over k will be dominated by its largest term, that is, the term minimizing $F_{w,n}$, under the constraints

$$
\int_0^\infty dk\, \rho(k) = N\,, \qquad \int_0^\infty dk\, k\,\rho(k) = n + \frac{N^2}{2}\,, \qquad 0 \leqslant \rho(k) \leqslant 1\,,
\tag{3.2}
$$

6

which fix the rank of the group $SU(N)$ and the number of atoms n, and implement the fact that the density of k_i can neither be negative nor exceed one, since $k_i - k_{i+1} \geqslant 1$. These constraints already suggest the scaling $N^2 \sim n$. We thus define the rescaled variable and parameters

$$x = \frac{k}{N}, \qquad t = \frac{4n}{N^2}, \qquad T_0 = \frac{c}{N} \tag{3.3}$$

and keep t, T_0 finite as $n, N \gg 1$ (the coefficient 4 in t is included to conform with the conventions of [18]). We also define a convenient temperature-dependent dimensionless parameter

$$x_T = \frac{tT}{4T_0}. \tag{3.4}$$

In terms of the above, the constraints become

$$\int_0^\infty dx\, \rho(x) = 1, \qquad \int_0^\infty dx\, x\, \rho(x) = \frac{t}{4} + \frac{1}{2}, \qquad 0 \leqslant \rho(x) \leqslant 1. \tag{3.5}$$

Also, the functional (3.1) becomes

$$\beta F_{w,n}[\rho(x)] = N^2 \left[-\frac{w}{2} \int_0^\infty dx \int_0^\infty dx'\, \rho(x)\rho(x') \ln|x - x'| \right.$$
$$\left. + \int_0^\infty dx\, \rho(x) \left(x(\ln x - 1) - \frac{x^2}{2x_T} \right) \right], \tag{3.6}$$

where we have neglected terms proportional to the constraints. We see that $F_{w,n}$ is indeed of order N^2, justifying the saddle point approximation. Enforcing the constraints (3.5) through similarly scaled Lagrange multipliers λ, μ, we need to extremize

$$\beta F_{w,n}[\rho(x)] + N^2\lambda \left(\int_0^\infty dx\, x\, \rho(x) - \frac{t}{4} - \frac{1}{2} \right) + N^2\mu \left(\int_0^\infty dx\, \rho(x) - 1 \right). \tag{3.7}$$

Variation in $\rho(x)$ gives

$$w \int_0^\infty dx'\, \rho(x') \ln|x - x'| = x(\ln x - 1) - \frac{x^2}{2x_T} + \lambda x + \mu. \tag{3.8}$$

Further differentiating (3.8) with respect to x we obtain

$$w \int_0^\infty dx'\, \frac{\rho(x')}{x - x'} = \ln x - \frac{x}{x_T} + \lambda. \tag{3.9}$$

The above equation must hold for x such that $0 < \rho(x) < 1$.

From (3.8) we see that the system corresponds to the equilibrium configuration of a large number N of particles with coordinates x_i repelling each other with a logarithmic potential $w \ln |x_i - x_j|$ inside an external potential $V_\lambda(x)$ given by the right hand side of (3.8), that is

$$V_\lambda(x) = x(\ln x - 1) - \frac{x^2}{2 x_T} + \lambda\, x + \mu \,. \tag{3.10}$$

Its derivatives

$$V_\lambda'(x) = \ln x - \frac{x}{x_T} + \lambda, \qquad V_\lambda''(x) = \frac{1}{x} - \frac{1}{x_T}\,, \tag{3.11}$$

indicate that, if $\lambda > \lambda_c$, where

$$\lambda_c = 1 - \ln x_T \,, \tag{3.12}$$

$V_\lambda(x)$ has a minimum at a value $x < x_T$ and a maximum at $x > x_T$ given by the solutions of

$$x\, e^\lambda = e^{x/x_T} \,, \tag{3.13}$$

while if $\lambda < \lambda_c$, $V_\lambda(x)$ is monotonically decreasing, as shown in fig. 1. So, for the potential to have a "well" able to retain particles, we need $\lambda > \lambda_c$. The solution of (3.9)
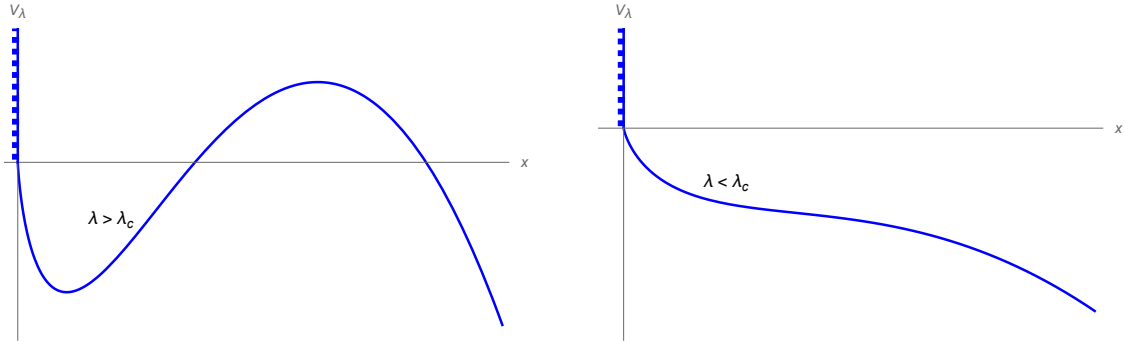

Figure 1: The potential $V_\lambda(x)$ (shifted by the constant μ) for a generic value of $\lambda > \lambda_c$ (left) and $\lambda < \lambda_c$ (right). It has a "rigid wall" at $x = 0$.

depends on whether the inequality constraint $\rho(x) \leqslant 1$ is saturated in a finite domain. The dilute phase correspond to the constraint not be saturated. This also means that the distribution $\rho(x)$ does not reach the "wall" on the left at $x = 0$, since the infinite potential there would force it to reach its saturation value $\rho(x) = 1$. Therefore, $\rho(x)$ is nonzero inside an interval $0 < a < x < b$ and vanishes outside (see fig. 2). Then solving (3.9) becomes a standard single-cut Cauchy problem. We define the resolvent

$$u(z) = w \int dx\, \frac{\rho(x)}{z - x}\,, \tag{3.14}$$

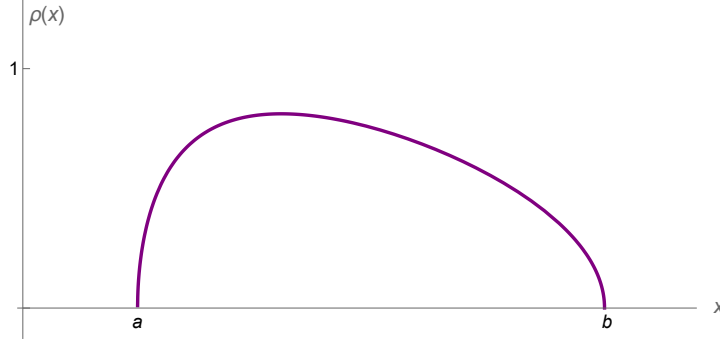with z on the upper complex plane. Its real and imaginary parts on the real axis

Figure 2: A typical shape of the distribution $\rho(x)$ in the dilute phase.

reproduce $\rho(x)$ and its Hilbert transform

$$u(x + i\epsilon) = w\!\!\!\!\fint dx' \frac{\rho(x')}{x - x'} - iw\pi\rho(x) . \tag{3.15}$$

Therefore, a function that is analytic on the upper half plane and its real part on the real axis equals $\ln x - x/x_T + \lambda$, as in (3.9), will equal $u(z)$ up to an additive constant, and its imaginary part will fix $\rho(x)$. In standard fashion, we write

$$u(z) = \frac{1}{2\pi i} \sqrt{(z-a)(z-b)} \oint ds\, \frac{\ln s - s/x_T + \lambda}{(s-z)\sqrt{(s-a)(s-b)}} , \tag{3.16}$$

where the contour winds in the clockwise direction around the cut of the square root but does not include the singularity at z and the cut of the logarithm (see fig. 3)
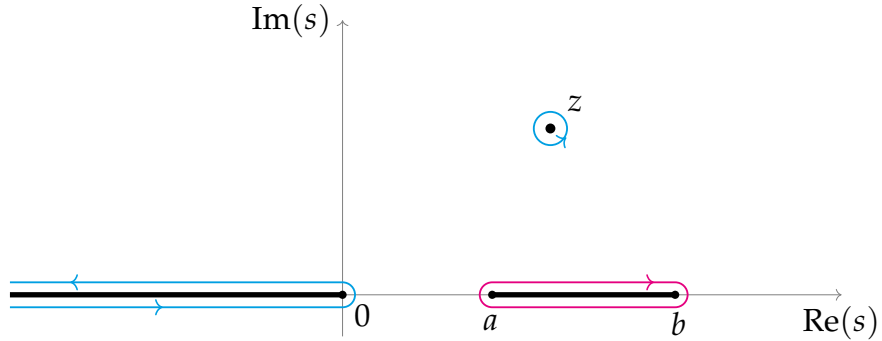

Figure 3: Contour of integration in the s-plane. The original (magenta) contour around the square root cut on (a, b) is pulled back to the two (cyan) contours around the pole at z and the logarithm cut on $(-\infty, 0)$. In addition, there is the contribution of the circle at infinity, taken clockwise, which is relevant for the linear in s term in the numerator of the integrand (3.16).

Pulling back the contour we pick up the pole at $s = z$ and the integrals around the cut

of the logarithm and infinity

$$u(z) = \ln z - \frac{z}{x_T} + \lambda$$

$$+ \frac{1}{x_T}\sqrt{(z-a)(z-b)} - \sqrt{(z-a)(z-b)}\int_0^\infty \frac{ds}{(s+z)\sqrt{(s+a)(s+b)}} \, .$$

(3.17)

Performing the integration we get that

$$u(z) = \ln z - \frac{z}{x_T} + \lambda$$

$$+ \frac{i}{x_T}\sqrt{(z-a)(b-z)} - i\cos^{-1}\frac{2z-a-b}{b-a} + i\cos^{-1}\frac{(a+b)z-2ab}{(b-a)z} \, .$$

(3.18)

For $z = x$ real and between a and b (the region in which $\rho(x)$ does not vanish) the last three terms are purely imaginary (the square root factor multiplying the integral provides a factor $+i$, since we assume that z approaches x from the upper-half complex plane). Then, according to (3.15), we determine $\rho(x)$ as

$$\rho(x) = \frac{1}{w\pi}\left(\cos^{-1}\frac{2x-a-b}{b-a} - \cos^{-1}\frac{(a+b)x-2ab}{(b-a)x}\right) - \frac{\sqrt{(x-a)(b-x)}}{w\pi x_T}$$

$$= \frac{2}{w\pi}\cos^{-1}\frac{\sqrt{x}+\sqrt{ab/x}}{\sqrt{a}+\sqrt{b}} - \frac{1}{w\pi x_T}\sqrt{(x-a)(b-x)}, \qquad a \leqslant x \leqslant b \, .$$

(3.19)

The second expression above makes clear that $\rho(x)$ vanishes at $x = a$ and $x = b$, and it never reaches or exceeds 1 if $w \geqslant 1$ (as we assume). Plotting the density (3.19) we indeed get a shape as in fig. 2 above. The parameters a, b and λ can be determined by matching the asymptotics of $u(z)$

$$u(z) = wz^{-1}\int_0^\infty dx\,\rho(x) + wz^{-2}\int_0^\infty dx\,x\,\rho(x) + \mathcal{O}(z^{-3})$$

$$= wz^{-1} + wz^{-2}\left(\frac{t}{4}+\frac{1}{2}\right) + \mathcal{O}(z^{-3}) \, ,$$

(3.20)

where in the second line we used (3.5). We obtain the conditions

$$2w = (\sqrt{b}-\sqrt{a})^2 - \frac{(a-b)^2}{4x_T} \, ,$$

$$w(t+2) = \frac{2(b-a)^2 + (\sqrt{b}-\sqrt{a})^4}{4} - \frac{(a-b)(a^2-b^2)}{4x_T} \, ,$$

(3.21)

$$\lambda = \frac{a+b}{2x_T} - 2\ln\frac{\sqrt{a}+\sqrt{b}}{2} \, .$$

10

To proceed, it is convenient to define two new parameters as

$$p = \frac{(\sqrt{a} + \sqrt{b})^2}{4x_T} , \quad q = \frac{(\sqrt{b} - \sqrt{a})^2}{4x_T} , \quad p > q > 0 , \tag{3.22}$$

with inverse

$$a = x_T(\sqrt{p} - \sqrt{q})^2 , \quad b = x_T(\sqrt{p} + \sqrt{q})^2 . \tag{3.23}$$

Then, the system (3.21) can be written more compactly as

$$2\bar{x}_T \, q(1 - p) = 1 ,$$

$$\bar{t} + 2 = 8\bar{x}_T^2 \, q\left(p + \frac{q}{2} - pq - p^2\right) \equiv g(p, q) , \tag{3.24}$$

$$\lambda = p + q - \ln(x_T p) .$$

where

$$\bar{x}_T = \frac{x_T}{w} = \frac{tT}{4wT_0} , \quad \bar{t} = \frac{t + 2}{w} - 2 , \tag{3.25}$$

thus eliminating w from the equations for p, q. Note that the first equation in (3.24) gives the stronger restriction $0 < q < p < 1$ for p and q.

In order for the above picture to be valid we should have $\lambda > \lambda_c$, where λ_c was defined in (3.12). This implies that

$$p - \ln p > 1 - q . \tag{3.26}$$

This is identically satisfied if (3.24) has real solutions. Indeed, since both p and q are positive, the left hand side of the inequality has a minimum of 1 at $p = 1$, while the right hand side is less than 1.

In addition, the density has to satisfy $0 \leqslant \rho(x) \leqslant 1$. Obviously, since the first term in (3.19) is bounded by unity and the second is negative, the density never exceeds unity. Nevertheless the density can become negative for a range of values of $x \in [a, b]$ rendering the solution unacceptable. Demanding that the derivatives of $\rho(x)$ at the end points at $x = a$ and $x = b$ are positive and negative, respectively, and recalling that $b > a$, we conclude that a necessary condition for having $\rho(x) \geqslant 0$ in the interval $x \in [a, b]$, is

$$x_T > \frac{1}{2}(b + \sqrt{ab}) \quad \Longrightarrow \quad p + \sqrt{pq} < 1 . \tag{3.27}$$

This condition is also sufficient for having $\rho(x) \geqslant 0$. Indeed, setting $\rho'(x) = 0$ gives

$$x^2 - x_T(1 + p + q)x + x_T{}^2(p - q) = 0 \,, \tag{3.28}$$

which has two real solutions for all values of the parameters in their range. Since $\rho(x)$ starts up with positive (negative) derivative at $x = a$ ($x = b$), where it vanishes, it cannot have two extrema between these values, and has just a single positive maximum. The condition (3.27) ensures that the largest root of (3.28), which corresponds to a negative minimum of $\rho(x)$, is larger than b and thus outside the range (a, b).

Solving for q the first equation in (3.24), the condition $p > q$ requires

$$p_- < p < p_+ \,, \qquad \bar{x}_T > 2 \,, \tag{3.29}$$

with

$$p_\pm = \frac{1 \pm \sqrt{1 - 2/\bar{x}_T}}{2} \,. \tag{3.30}$$

Then (3.27) becomes

$$f(p) \equiv p + \sqrt{\frac{p}{2\bar{x}_T(1 - p)}} - 1 < 0 \,. \tag{3.31}$$

The function $f(p)$ is increasing, and we can see that

$$f(p_\pm) = \pm\sqrt{1 - \frac{2}{\bar{x}_T}} \,. \tag{3.32}$$

Therefore, (3.31) holds for

$$p_- < p < p_0 < p_+ \,, \qquad \bar{x}_T > 2 \,, \qquad f(p_0) = 0 \,, \tag{3.33}$$

which is a refinement of (3.29). The value of p_0 can be calculated analytically and arises from a cubic equation with one real solution given by

$$p_0 = 1 - 6^{-1/3}\zeta^{-1} + 6^{-2/3}\bar{x}_T^{-1}\zeta \,, \qquad \zeta = \left(\sqrt{6\bar{x}_T^3 + 81\bar{x}_T^4} - 9\bar{x}_T^2\right)^{1/3} \,, \tag{3.34}$$

and monotonically increases from $1/2$ to 1 in the interval $\bar{x}_T \in [2, \infty)$ and is always bounded by p_+.

Finally, the function $g(p) = g(p, q(p))$ defined in the second equation of (3.24), after

eliminating q using (3.24), becomes

$$g(p) = \frac{1 - 2p}{(1 - p)^2} + 4\bar{x}_T p . \tag{3.35}$$

Moreover, since

$$g'(p) = 4\bar{x}_T - \frac{2p}{(1 - p)^3} , \tag{3.36}$$

we easily see that $g'(p_0) = 0$. Since $g''(p) < 0$ the function $g(p)$ has a maximum at $p = p_0$. It is easily checked that $g(p_-) > 0$ and therefore $g(p) > 0$ and increasing in $p \in [p_-, p_0]$. Consequently, the second of (3.24) has a unique solution in p for $\bar{t}$ in the range

$$g(p_-) < \bar{t} + 2 < g(p_0) \tag{3.37}$$

and no solutions outside this range, signaling a transition to different phases. For $g(p_-)$ we may use the expression

$$g(p_-) = 2\left(3\bar{x}_T - \bar{x}_T^2 + \sqrt{\bar{x}_T(\bar{x}_T - 2)^3} \right) . \tag{3.38}$$

In addition, $g(p_0)$ can be computed to be

$$g(p_0) = \frac{4p_0^2 - 3p_0 + 1}{(1 - p_0)^3} , \tag{3.39}$$

where p_0 is given by (3.34).

The condition $\bar{t} + 2 > g(p_-)$ in (3.37) derives from $p > q$, that is, $a > 0$. Saturating it implies $a = 0$ and signals a transition to a dense phase, in which $\rho(x)$ extends to $x = 0$ and starts saturating to $\rho(x) = 1$. Therefore, $\bar{t} + 2 = g(p_-)$ identifies the critical temperature T_c at which the transition happens.[3] Working out the details of this equation we get a second order algebraic equation for T whose positive solution is the critical temperature

$$T_c = 2wT_0 \frac{3t + 6 - 8w + w^{-1/2}\left(4w - 2 - t\right)^{3/2}}{t(t - 3w + 2)} , \tag{3.40}$$

$$3w - 2 \leqslant t \leqslant 4w - 2 \quad (1 \leqslant \bar{t} \leqslant 2) ,$$

---

[3]Physically, to be in the dilute phase we should have $T > T_c$. This can also be seen algebraically by expanding the left hand side of the inequality $g(p_-) - \bar{t} - 2 < 0$ near $T = T_c$. To leading order this is proportional to $\left(g'(p_-)\frac{dp_-}{d\bar{x}_T}\Big|_{T_c} + 4p_- \right)(T - T_c) < 0$. The coefficient of $T - T_c$ is negative and therefore $T > T_c$ as stated.

where we have also used (3.25). The critical temperature T_c is monotonically decreasing with t, from $T_c \to \infty$ as $t \to 3w - 2$, consistent with the result of [17], to $T_c = 4wT_0/(2w - 1)$ for $t = 4w - 2$. If particular, near $t = 4w - 2$, we have the expansion

$$T_c = T_0 \frac{4w}{2w - 1} - T_0 \frac{4w - 1}{(2w - 1)^2}(t - 4w + 2) + \dots \,. \tag{3.41}$$

and near $t = 3w - 2$ the behavior

$$T_c = T_0 \frac{4w^2}{3w - 2} \frac{1}{t - 3w + 2} + \dots \,. \tag{3.42}$$

Finally, note that the corresponding critical value for b is

$$b_c = 4w - 2\sqrt{w}\sqrt{4w - 2 - t} \,. \tag{3.43}$$

It increases with t, from $b_c = 2w$ as $t \to 3w - 2$, to $b_c = 4w$ for $t = 4w - 2$.

The condition $\bar{t} + 2 < g(p_0)$ in (3.37) derives from the positivity of the density ρ and, when saturated, signals an instability: the distribution $\rho(x)$ cannot be lumped and, instead, one isolated k_i moves over the hump of the potential to a large value of k. Therefore, $\bar{t} + 2 = g(p_0)$ identifies another critical temperature T_s that marks the onset of instability and the transition to a disjoint phase.[4] Using (3.39) we have an explicit expression of t in terms of T_s which is hard to invert. To proceed we recall that

$$2\bar{x}_T = \frac{p_0}{(1 - p_0)^3} \tag{3.44}$$

and reparametrize as

$$p_0 = \frac{s}{s + 1} \quad \implies \quad 2\bar{x}_T = s(s + 1)^2 \,. \tag{3.45}$$

Note that, (3.44) and the first of (3.24) amount to saturating the constraint in (3.27). Proceeding, the condition $g(p_0) = \bar{t} + 2$ upon using (3.39) and (3.45) gives

$$s^2(2s + 1) = \bar{t} + 1 \,, \tag{3.46}$$

---

[4] Again for $T > T_s$ we are in the dilute phase. This can be seen also be seen by expanding the right hand side of the inequality $g(p_0) - \bar{t} - 2 > 0$ near $T = T_s$. To leading order this is proportional to $\left(g'(p_0)\frac{dp_0}{d\bar{x}_T}\Big|_{T_s} + 4p_0\right)(T - T_s) > 0$. The coefficient of $T - T_s$ is positive and therefore $T > T_s$ as stated.

14

with primary solution

$$s = \frac{1}{6}\left(\delta + \delta^{-1} - 1\right) , \qquad \delta = \left(\sqrt{(54\bar{t}+53)^2 - 1} + 54\bar{t} + 53\right)^{1/3} . \tag{3.47}$$

Plugging in (3.45), gives the critical temperature T_s as

$$T_s = T_0\frac{w}{12t}\left(\delta^2 + 2\delta + 2\delta^{-1} + \delta^{-2} + 12\bar{t} + 11\right) , \quad t \geqslant 4w - 2 \quad (\bar{t} \geqslant 2) . \tag{3.48}$$

Note that, for $t = 4w - 2$, we have the expansion

$$T_s = T_0\frac{4w}{2w-1} - T_0\frac{t + 2 - 4w}{(2w-1)^2} + \dots . \tag{3.49}$$

Therefore, T_s joins T_c at the highest t for which T_c is defined albeit with a first derivative discontinuity as it can be seen by the expansions (3.41) and (3.49). On the other hand, $T_s(t)$ for $t < 4w - 2$ does not make sense, since it enters the region $T < T_c$ in which the lumped solution does not hold. For $t \to \infty$, T_s slowly asymptotes to T_0 as

$$T_s = T_0 + 3T_0\left(\frac{w}{4t}\right)^{1/3} + \dots . \tag{3.50}$$

4   Lumped dense distributions

Below the critical temperature T_c, the distribution $\rho(x)$ touches $x = 0$ and the dilute solution is not valid any more. A finite part of the distribution will condense to the maximal value $\rho = 1$ near $x = 0$, and the equilibrium conditions for the remaining $\rho < 1$ part are modified. Assuming that $\rho(x)$ condenses for $0 < x < a$, and vanishes for $x > a + b$, we set

$$\rho(x) = \begin{cases} 1 , & 0 < x < a , \\ \rho_0(x - a) , & a < x < a + b , \end{cases} \tag{4.1}$$

and zero elsewhere, with a and b positive constants (see fig. 4). The constraints (3.5) become

$$0 \leqslant \rho_0(x) \leqslant 1 , \quad \int_0^b dx\, \rho_0(x) = 1 - a , \quad \int_0^b dx\, x\, \rho_0(x) = \frac{t}{4} + \frac{(1-a)^2}{2} . \tag{4.2}$$

Substitution of $\rho(x)$ in (3.6) yields, upon changing variable $x \to x + a$,

15
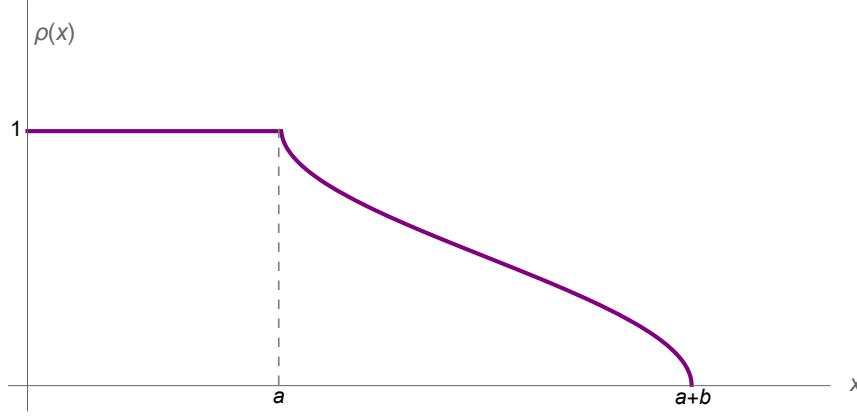
Figure 4: A typical shape of the distribution $\rho(x)$ in the dense phase.

$$\beta F_{w,n}[\rho_0(x)] = N^2 \left[-\frac{w}{2} \int_0^\infty dx \int_0^\infty dx' \, \rho_0(x)\rho_0(x') \ln|x - x'| \right.$$

$$+ \int_0^\infty dx \, \rho_0(x) \left(wx(\ln x - 1) - \frac{x^2}{2x_T} \right) \qquad (4.3)$$

$$\left. -(w - 1) \int_0^\infty dx \, \rho_0(x) \, (x + a) \big(\ln(x + a) - 1 \big) \right] ,$$

where we omitted terms that are set to constants by the constraints. Implementing the constraints (4.2) with appropriate Lagrange multipliers and minimizing the effective action leads to the equilibrium equation

$$w \int_0^\infty dx' \, \rho_0(x') \ln|x - x'| = wx(\ln x - 1) - (w - 1)(x + a)\big(\ln(x + a) - 1 \big)$$

$$(4.4)$$

$$- \frac{x^2}{2x_T} + \lambda x + \mu .$$

Taking the x-derivative we obtain the analog of (3.9), i.e.,

$$w \int_0^\infty dx' \frac{\rho_0(x')}{x - x'} = w \ln x - (w - 1) \ln(x + a) - \frac{x}{x_T} + \lambda , \qquad (4.5)$$

when $\rho_0(x) > 0$. We see that now the equation for $\rho_0(x)$ has a two-logarithm potential, given by the right hand side of (4.4) as

$$V_{\lambda,w,a}(x) = w\,x(\ln x - 1) - (w - 1)(x + a)\Big(\ln(x + a) - 1 \Big) - \frac{x^2}{2x_T} + \lambda x + \mu , \quad (4.6)$$

while for $w = 1$ the second logarithm drops out.

16

To solve for $\rho_0(k)$, we define as before the resolvent

$$u_0(z) = w \int dk \, \frac{\rho_0(k)}{z - k} \, , \qquad (4.7)$$

reproducing $\rho_0(k)$ and its Hilbert transform as

$$u_0(k + i\epsilon) = w \!\!\!\!\fint dk' \frac{\rho_0(k')}{k - k'} - iw\pi\rho_0(k) \, . \qquad (4.8)$$

In analogy to (3.16), we set

$$u_0(z) = \frac{1}{2\pi i} \sqrt{z(z - b)} \oint ds \, \frac{w \ln s - (w - 1) \ln(s + a) + \lambda - s/x_T}{(s - z)\sqrt{s(s - b)}} \, , \qquad (4.9)$$

where the contour winds in the clockwise direction around the cut of the square root $[0, b]$ but does not include the singularity at z nor the cuts of the logarithms (so it "threads" the real line at $k = 0$, see fig. 5).
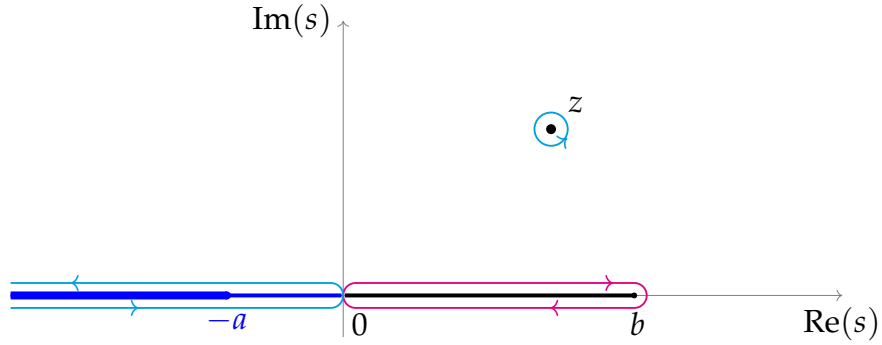

Figure 5: Contour of integration in the s plane. The original (magenta) contour around the (black) square root cut on $(0, b)$ is pulled back to the two (cyan) contours around the pole at z and the two (blue) logarithm cuts on $(-\infty, -a)$ and $(-a, 0)$.

Pulling back the contour we pick up the pole at $s = z$ and the integrals around the cuts of the logarithms and around infinity, and obtain

$$u_0(z) = w \ln z - (w - 1) \ln(z + a) - \frac{z}{x_T} + \lambda + \frac{1}{x_T}\sqrt{z(z - b)}$$
$$- \sqrt{z(z - b)} \left[w \int_0^a + \int_a^\infty \right] \frac{ds}{(s + z)\sqrt{s(s + b)}} \, . \qquad (4.10)$$

For $z = x$ real and between 0 and b (the region in which $\rho_0(x)$ does not vanish) we obtain for $\rho_0(x)$

$$\rho_0(x) = \sqrt{x(b - x)} \left[\int_0^a + \frac{1}{w} \int_a^\infty \right] \frac{ds}{(s + x)\sqrt{s(s + b)}} - \frac{1}{\pi w x_T}\sqrt{x(b - x)} \qquad (4.11)$$

17

and upon performing the integrals,

$$\rho_0(x) = \frac{2}{w\pi}\cos^{-1}\sqrt{\frac{x}{b}} + \frac{2(w-1)}{w\pi}\cos^{-1}\sqrt{\frac{(a+b)x}{(a+x)b}} - \frac{1}{\pi w x_T}\sqrt{x(b-x)}. \quad (4.12)$$

The density $\rho_0(x)$ obeys $\rho_0(0) = 1$ and $\rho_0(b) = 0$. The parameters a, b and λ can be related to N and n by matching the asymptotic expansion of $u_0(z)$

$$u_0(z) = wz^{-1}\int_0^\infty dx\,\rho_0(x) + wz^{-2}\int_0^\infty dx\,x\,\rho_0(x) + \mathcal{O}(z^{-3})$$

$$= wz^{-1}(1-a) + wz^{-2}\left(\frac{t}{4} + \frac{(1-a)^2}{2}\right) + \mathcal{O}(z^{-3}), \quad (4.13)$$

obtained from (4.7,4.2) to those obtained from (4.9). We get

$$1-a = \frac{b}{2} - \frac{w-1}{2w}\left(\sqrt{a+b}-\sqrt{a}\right)^2 - \frac{b^2}{8wx_T},$$

$$\frac{t}{2} + (1-a)^2 = \frac{3b^2}{8} + \frac{w-1}{2w}\left(-\frac{3b^2}{4} + 2a^2 + (b-2a)\sqrt{a(a+b)}\right) - \frac{b^3}{8wx_T}, \quad (4.14)$$

$$\lambda = 2(w-1)\ln\frac{\sqrt{a}+\sqrt{a+b}}{2} - w\ln\frac{b}{4} + \frac{b}{2x_T}.$$

We note that, for $a = 0$, the equations (4.14) in the dense phase and (3.21) in the dilute phase become identical, since b and λ are continuous at the transition between the two phases, which happens at the critical temperature T_c in (3.40).

The second critical temperature T_s signaling the onset of instability occurs when $\rho_0(x)$ in (4.12) develops a negative part. Its extrema, happening at $\rho_0'(x) = 0$, satisfy

$$x^2 + \left(a - \frac{b}{2} - x_T\right)x - a\left(\frac{b}{2} + x_T\right) - (w-1)x_T\sqrt{a(a+b)} = 0. \quad (4.15)$$

The smaller root x_- is always negative and outside of the range of x $[0,b]$. The positive root x_+ can be inside the range and corresponds to a negative minimum. Stability is ensured if $x_+ > b$, giving the condition

$$2x_T > \frac{b\sqrt{a+b}}{\sqrt{a+b} + (w-1)\sqrt{a}}. \quad (4.16)$$

The critical point is at $x_+ = b$, which means that the above inequality is saturated,

thus allowing to express the parameter a as

$$\text{at criticality :} \qquad a = \frac{b(b - 2x_T)^2}{(2wx_T - b)(2(w-2)x_T + b)}, \qquad w \neq 1. \qquad (4.17)$$

Substituting the value (4.17) for a in the first two equations in (4.14) determines b and $T_{s'}$. The equations are of high order and, in general, can only be solved numerically. It turns out that $T_{s'}$ joins T_c and T_s for the dilute case at $t = 4w - 2$, forming a triple critical point on the (t, T)-plane, located at

$$\text{Triple point :} \qquad t = 4w - 2, \quad T = \frac{4w}{2w - 1} T_0. \qquad (4.18)$$

Moreover, it turns out that T_s and $T_{s'}$ have their first derivatives (but not necessarily higher ones) continuous at $t = 4w - 2$ and therefore join smoothly at this point. Hence, we may think of them as a single curve over the entire range of values of t, which we will denote by T_s, having different functional forms on either side of $t = 4w - 2$.

5 The disjoint phase

When $T < T_s$, either in the dilute or the dense lumped phase, the distribution develops a negative part, signaling an instability. The stable configuration consists of a single k_i (the largest one) leaving the distribution and moving to a large value, as we shall see. Since the k_i are ordered, we take this to be k_1. The remaining k_i are treated using a distribution $\rho(k)$ as before.

It is clear that the contribution of the single isolated k_1 to the equilibrium equation for the remaining k_i and their density $\rho(k)$ is subleading in N. The only way that it can influence the distribution is through the constraints (3.2), which become

$$\int_0^\infty dk\, \rho(k) = N - 1 \simeq N, \qquad \int_0^\infty dk\, k\, \rho(k) = n + \frac{N^2}{2} - k_1. \qquad (5.1)$$

This implies that k_1 must be of order N^2, and we set

$$k_1 = N^2 y, \qquad (5.2)$$

contrasted to $k_i = Nx_i$ for the rest of the k_i. The equilibrium equations for $\rho(x)$ and y

19

become

$$\frac{w}{Nx - N^2 y} + w \int_0^\infty dx' \frac{\rho(x')}{x - x'} = \ln x - \frac{x}{x_T} + \lambda \tag{5.3}$$

and

$$w \int_0^\infty dx \frac{\rho(x)}{Ny - x} = \ln(Ny) - \frac{Ny}{x_T} + \lambda , \tag{5.4}$$

where we also displayed the subleading terms. In addition, the constraints for $\rho(x)$ become

$$\int_0^\infty dx\, \rho(x) = 1 , \qquad \int_0^\infty dx\, x\, \rho(x) = \frac{t}{4} + \frac{1}{2} - y . \tag{5.5}$$

From (5.3) we see that, indeed, y does not influence the equation for ρ, as the y-dependent term is of order $1/N^2$. Keeping leading terms in N, (5.4) implies

$$\lambda = N \frac{y}{x_T} , \tag{5.6}$$

so that λ assumes a macroscopically large (of order N) positive value. This drives the configuration for ρ deep into the dense phase, that is,[5] (see fig. 6)
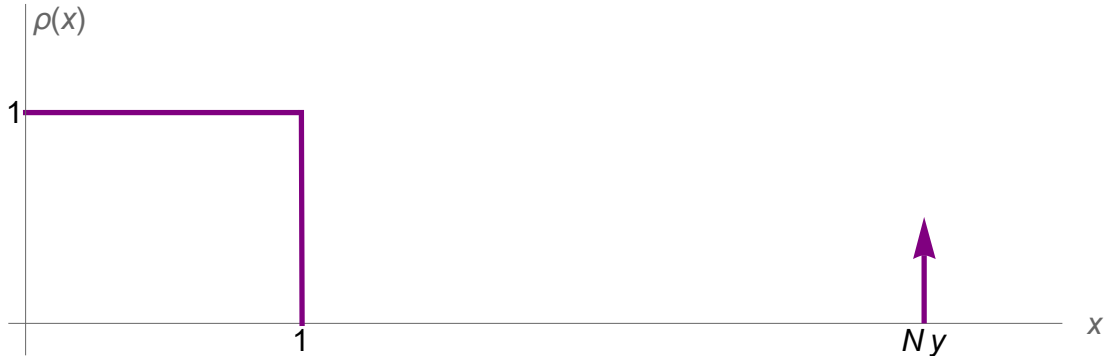

Figure 6: The distribution $\rho(x)$ in the disjoint phase with one isolated $x_1 = Ny$.

$$\rho(x) = \begin{cases} 1, & 0 \leqslant x \leqslant 1, \\ 0, & \text{otherwise}, \end{cases} \tag{5.7}$$

and the second constraint in (5.5) gives

$$y = \frac{t}{4} . \tag{5.8}$$

---

[5]That (5.7) and (5.8) are the solution to (5.3)-(3.5) to leading order in N also arises from the system (4.14) in the lumped dense phase upon shifting $t/2 \to t/2 - 2y$, which takes into account the presence of the separate eigenvalue k_1 that modifies (5.1) as compared to (3.2). For large λ the last of (4.14) implies that $b \to 0$. Then, the first two equations give $(1 - a)^2 + t/2 - y/2 + \mathcal{O}(b^2) = 0$ and $1 - a + \mathcal{O}(b) = 0$, which implies that $a = 1$ and $y = t/4$ as above and the distribution (4.1) becomes the one of (5.7).

Therefore, the disjoint phase consists of a fully condensed distribution $\rho(x)$ and a single large isolated $k_1 = Nx_1 = N^2t/4 = n$, the remaining k_i ranging from 0 to $N-2$. The corresponding irrep is the fully symmetric one with a single row of length n in its Young tableau, so we will refer to the disjoint phase as the symmetric phase.

We conclude by noting that, had we separated two or more large k_i, e.g., k_1 and k_2, we could not have fulfilled the equilibrium condition. In the situations above, k_1 is sitting at the top of the effective potential to leading order in N (to subleading order, slightly to the left, stabilized by the repulsion of the lumped set $\rho(x)$). More than one k_i would repel each other and could not stabilize. This is in accordance with the findings of [17] where it was shown that, for finite N, configurations with two or more rows in their Young tableaux lead to instabilities.

The full phase diagram, obtained after deriving the corresponding phase transitions in section 7, is depicted in fig. 7.

6   The special cases $w = 1$ and $w = 2$

As we mentioned in section 2 on the general model, the cases $w = 1$ and $w = 2$ are special: $w = 1$ corresponds to simply enumerating irreducible components, while $w = 2$ is the standard thermodynamic model where all states are counted with equal weight. As demonstrated in [18] these values are also special from the mathematical point of view: in the absence of the energy term (when $T \to \infty$), they both admit simple, explicit solutions for the equilibrium configuration and its parameters a, b. Moreover, the dense-dilute phase transition in the parameter t is third order for $w = 1$, and completely absent for $w = 2$, while for generic $w > 1$ it is fourth order. We therefore examine the present model in these two special cases.

6.1 $w = 1$

In this case the density in the dense phase (4.12) specializes to

$$\text{Dense}: \quad \rho_0(x) = \frac{2}{\pi}\cos^{-1}\sqrt{\frac{x}{b}} - \frac{1}{\pi x_T}\sqrt{x(b-x)}, \qquad 0 \leqslant x \leqslant b, \qquad (6.1)$$

which obeys $\rho_0(0) = 1$ and $\rho_0(b) = 0$. This distribution remains in the physical range $0 \leqslant \rho_0(x) \leqslant 1$ for all values of $x \in [0, b]$ as long as

$$2x_T > b \, , \tag{6.2}$$

which follows by setting $w = 1$ in (4.16). The equations determining the parameters a, b and λ (4.14) simplify to

$$
\begin{aligned}
1 - a &= \frac{b}{2} - \frac{b^2}{8x_T} \, , \\
\frac{t}{4} + \frac{(1-a)^2}{2} &= \frac{3b^2}{16} - \frac{b^3}{16x_T} \, , \\
\lambda &= -\ln\frac{b}{4} + \frac{b}{2x_T} \, .
\end{aligned}
\tag{6.3}
$$

This system can be solved for a and b by elimination, leading to a quadratic equation for b^2. The unique positive solution satisfying the condition (6.2) for the distribution $\rho_0(x)$ to remain in the physical range, is given by $b = 2x_T\sqrt{1 - \sqrt{1 - 2t/x_T^2}}$. Then, a and λ are obtained from the first and last equations in (6.3). We are mostly interested in the expressions for the critical temperatures T_c and T_s which can be explicitly calculated. The former is obtained by setting $a = 0$, which signals a transition to a dilute phase. From (6.3) we obtain

$$T_c = 2T_0 \frac{3t - 2 + (2 - t)^{3/2}}{t(t-1)} \, , \qquad 1 \leqslant t \leqslant 2 \, , \tag{6.4}$$

which of course is consistent with (3.40) for $w = 1$ as it should be. The other critical temperature T_s is obtained by setting b to its critical value which, according to (6.2) is at $b = 2x_T$. The first equation in (6.3) fixes $a = 1 - x_T/2$, and the second equation determines the critical temperature as

$$T_s = T_0\sqrt{\frac{32}{t}} \, , \qquad t \leqslant 2 \, . \tag{6.5}$$

The range of t is determined by demanding $a \geqslant 0$. For $t = 2$, indeed $T_s = 4T_0$. Also, $T > T_s$ warrants that the expression for b given below (6.3) remains real.

For the dilute phase, $\rho(x)$ is given by (3.19) for $w = 1$ which we reproduce for

22

convenience here

Dilute : $\quad \rho(x) = \dfrac{2}{\pi} \cos^{-1} \dfrac{\sqrt{x} + \sqrt{ab/x}}{\sqrt{a} + \sqrt{b}} - \dfrac{1}{\pi x_T} \sqrt{(x-a)(b-x)}, \quad a \leqslant x \leqslant b.$ (6.6)

The constants a, b, λ are determined by (3.21) for $w = 1$, with no substantial simplifi-
cation. The critical temperature for transition to the disjoint phase is given by (3.48)
for $w = 1$ and $\bar{t} = t$, that is

$$T_s = \dfrac{T_0}{12t} \left(\delta^2 + 2\delta + 2\delta^{-1} + \delta^{-2} + 12t + 11 \right),$$

$$\delta = \left(\sqrt{(54t+53)^2 - 1} + 54t + 53 \right)^{1/3}, \qquad t \geqslant 2.$$

(6.7)

Its value and first derivative (but not the higher ones) match those of T_s in the dense
phase (6.5) above for $t = 2$, the two curves essentially joining into one continuous
curve for all values of t.

6.2 $\quad w = 2$

In this case a particular simplification and unification between the dense and dilute
phases arises. The density in the dense phase (4.12) specializes to

$$\rho_0(x) = \dfrac{1}{\pi} \cos^{-1} \dfrac{(1 + \sqrt{1 + b/a})x - b}{b\sqrt{1 + x/a}} - \dfrac{1}{2\pi x_T} \sqrt{x(b-x)}, \qquad 0 \leqslant x \leqslant b. \quad (6.8)$$

It obeys $\rho_0(0) = 1$ and $\rho_0(b) = 0$, and remains in the physical range $0 \leqslant \rho_0(x) \leqslant 1$, for
all values of $x \in [0, b]$ as long as

$$2x_T > a + b - \sqrt{a(a+b)},$$ (6.9)

which follows by setting $w = 2$ in (4.16). The system of equations (4.14) becomes

$$4 = \left(\sqrt{a+b} + \sqrt{a} \right)^2 - \dfrac{b^2}{4x_T},$$

$$\dfrac{t}{2} + (1-a)^2 = \dfrac{3b^2}{16} + \dfrac{a^2}{2} + \dfrac{b-2a}{4} \sqrt{a(a+b)} - \dfrac{b^3}{16x_T},$$

$$\lambda = \dfrac{b}{2x_T} - 2\ln \dfrac{\sqrt{a+b} - \sqrt{a}}{2}.$$

(6.10)

The density in the dilute phase (3.19) specializes to

$$\rho(x) = \frac{1}{\pi} \cos^{-1} \frac{\sqrt{x} + \sqrt{ab/x}}{\sqrt{a} + \sqrt{b}} - \frac{1}{2\pi x_T} \sqrt{(x-a)(b-x)} , \qquad a \leqslant x \leqslant b , \qquad (6.11)$$

which obeys $\rho(a) = \rho(b) = 0$, and remains in the physical range $0 \leqslant \rho(x) \leqslant 1$ for all values of $x \in [a, b]$ as long as (3.27) holds. Repeated here for convenience this reads

$$2x_T > b + \sqrt{ab} . \qquad (6.12)$$

The system of equations (3.21) becomes

$$4 = (\sqrt{b} - \sqrt{a})^2 - \frac{(b-a)^2}{4x_T} ,$$

$$2(t+2) = \frac{2(b-a)^2 + (\sqrt{b} - \sqrt{a})^4}{4} - \frac{(a-b)(a^2 - b^2)}{4x_T} , \qquad (6.13)$$

$$\lambda = \frac{a+b}{2x_T} - 2\ln \frac{\sqrt{a} + \sqrt{b}}{2} .$$

The critical temperature T_c for transition between the two phases is given by (3.40) as

$$T_c = 4T_0 \frac{3t - 10 + 2^{-1/2}(6-t)^{3/2}}{t(t-4)} , \qquad 4 \leqslant t \leqslant 6 . \qquad (6.14)$$

The two systems (6.10) and (6.13)), and the constraints (6.9) and (6.12), become, in fact, identical upon using the p, q-parametrization:

$$\text{Dense phase:} \quad a = x_T(\sqrt{p} - \sqrt{q})^2 , \quad b = 4x_T\sqrt{pq} , \quad p < q ,$$
$$\text{Dilute phase:} \quad a = x_T(\sqrt{p} - \sqrt{q})^2 , \quad b = x_T(\sqrt{p} + \sqrt{q})^2 , \quad p > q . \qquad (6.15)$$

Their common form is, upon combining the top two equations in (6.10),

$$x_T q(1 - p) = 1 ,$$

$$2x_T^2(q^2 - 2pq(p + q - 1)) = t + 2 ,$$

$$\lambda = p + q - \theta(q - p)(\sqrt{p} - \sqrt{q})^2 - \ln(x_T p) , \qquad (6.16)$$

$$p + \sqrt{pq} < 1 ,$$

where θ is the Heaviside step function. For $T > T_c$ the solution of (6.16) is for $p > q$, while for $T < T_c$ it is for $p < q$. So the transition is completely analytic, the only sign

24

of nonanalyticity being the Heaviside step function in the expression for the Lagrange multiplier λ. This will be relevant in the study of the order of the transition. The critical temperature T_s for transition into the disjoint phase is given by (3.48) for $w = 2$, which are now valid for both the dense and dilute phases. Specifically,

$$T_s = \frac{T_0}{6t}\left(\delta^2 + 2\delta + 2\delta^{-1} + \delta^{-2} + 6t - 1\right),$$

$$\delta = \left(\sqrt{(27t-1)^2 - 1} + 27t - 1\right)^{1/3}, \qquad t \geqslant 0.$$

(6.17)

This diverges at $t = 0$ as $T_s \simeq T_0\sqrt{8/t}$ and slowly asymptotes to $T_s = T_0$ as $t \to \infty$. At the triple point, $t = 6$, $T_s = T_c = 8T_0/3$. The plots of T_c, T_s are given in fig. 7.

7 Thermodynamics and phase transitions

The free energy F, internal energy U, and entropy S in each phase are related by the standard thermodynamic relations

$$F = U - TS, \qquad U = -T^2\partial_T\left(\frac{F}{T}\right), \qquad S = -\partial_T F.$$

(7.1)

The critical temperatures T_c and T_s define transition lines on the (t, T) plane, with a triple point given in (4.18). To determine the order of these phase transitions, we examine the thermodynamic quantities of each phase.

7.1 Transitions between the dilute and dense phases

For the dense and dilute cases, the expression (3.6) for the free energy in terms of the distribution $\rho(x)$ identifies the entropy and internal energy as

$$S = N^2\left[\frac{w}{2}\int_0^\infty dx \int_0^\infty dx'\, \rho(x)\rho(x')\ln|x - x'| - \int_0^\infty dx\, \rho(x)x(\ln x - 1)\right],$$

$$U = -2N^2\frac{T_0}{t}\int_0^\infty dx\, x^2\rho(x),$$

(7.2)

calculated at the equilibrium configuration $\rho(x)$. Substituting the explicit expressions (3.19) in the dilute case, or (4.12) in the dense phase, leads to some hard to evaluate integrals, even after using the equilibrium equation (3.8) to simplify S. However, U can

25

be calculated from the asymptotic expansion of the resolvent $u(z)$, as it is essentially the second moment of the distribution. This will allow us to determine the order of the dense-dilute phase transition. Note that both U and S, and consequently also F, are of order N^2.

For the lumped dilute phase, keeping one more term in the expansion (3.20), of order z^{-3}, we obtain

$$w \int_0^\infty dx\, x^2 \rho(x) = \frac{5(a^3 + b^3) + 3ab(a + b) - 2\sqrt{ab}(3a^2 + 2ab + 3b^2)}{48}$$
$$- \frac{(a - b)^2(5a^2 + 6ab + 5b^2)}{128 x_T} . \tag{7.3}$$

Similarly, for the lumped dense phase we obtain

$$w \int_0^\infty dx\, x^2 \rho(x) = \frac{w}{3}a^3 + \frac{5b^3}{48} - \frac{5b^4}{128 x_T} + \frac{w - 1}{24}\frac{\sqrt{a}\, b^3(11a + 3b + 9\sqrt{a(a + b)})}{(\sqrt{a} + \sqrt{a + b})^3} , \tag{7.4}$$

where the first term comes from the unit part of the distribution in (4.1) and the rest from the nontrivial profile $\rho_0(x)$.

We need to expand the above expressions in the temperature near the phase boundary at $T = T_c$, corresponding to $a = 0$. To do this, we expand a and b in $T - T_c$, which can be done by perturbatively solving the first two equations in (3.21) and (4.14). This expansion is qualitatively different for $w = 1$ and $w > 1$: in the generic case $w > 1$, the two sets of equations allow for an expansion of $\sqrt{a}$ and b in powers of $T - T_c$ around their critical values $a = 0$ and $b = b_c$. However, for $w = 1$, the terms involving $\sqrt{a}$ in (4.14) drop, and the variables to expand in the dense phase are a and b. As we shall see, this also affects the order of the transition. Hence, we treat separately the cases $w = 1$ and $w > 1$.

7.1.1 $w = 1$: 2$^{\text{nd}}$ order phase transition

First we consider the dilute phase and the system (3.21) with $w = 1$. It turns out that it suffices to keep terms of $\mathcal{O}(T - T_c)$ in the expansion of $\sqrt{a}$ and b. We find the

expansion

$$\sqrt{a} = \frac{1}{4\sqrt{2}T_0} \frac{t(1-\sqrt{2-t})^2}{(2-\sqrt{2-t})^{5/2}}(T-T_c) + \dots ,$$

$$b = b_c + \frac{t(1-t)(1-\sqrt{2-t})}{2(2-t(1-\sqrt{2-t}))T_0}(T-T_c) + \dots ,$$

(7.5)

from which the internal energy obtains as

$$U_{\text{dil}} = U_0 + \frac{N^2}{4}(1-\sqrt{2-t})^2(T-T_c) + \dots ,$$

(7.6)

where the internal energy at $T = T_c$ is

$$U_0 = -\frac{5N^2}{12}T_c(t-1) .$$

(7.7)

This is negative, in accordance with (7.2), since approaching the critical curve $T = T_c$ requires that $1 \leqslant t \leqslant 2$.

In the dense phase and the system (6.3) we keep terms of $\mathcal{O}(T-T_c)$ in the expansion of a and b. We find that

$$a = -\frac{1}{2T_0} \frac{t(1-\sqrt{2-t})^2}{(2-\sqrt{2-t})(4-3\sqrt{2-t})}(T-T_c) + \dots ,$$

$$b = b_c + \frac{(2-7t+t^2)\sqrt{2-t}+t(2+5t-3t^2)}{(t^2-4)(2-9t)T_0}(T-T_c) + \dots ,$$

(7.8)

from which

$$U_{\text{den}} = U_0 - \frac{5N^2}{4} \frac{\sqrt{2-t}(1-\sqrt{2-t})^2}{4-3\sqrt{2-t}}(T-T_c) + \dots .$$

(7.9)

Comparing (7.6) and (7.9) we see that there is a discontinuity in the first derivative of the internal energy with respect to T at the critical temperature T_c. This corresponds to a second order phase transition.

Note that the internal energy, as stated in (7.6) and (7.9), is an increasing (decreasing) function of the temperature off the critical curve $T = T_c$ for the dilute (dense) phase.

7.1.2 $w > 1$: 3$^{\text{rd}}$ order phase transition

In this case we will need to expand to order $\mathcal{O}(T - T_c)^2$. For the dilute phase, we find

$$\sqrt{a} = \frac{b_c^{3/2}T_0}{4tT_c^2}(T - T_c) + \frac{b_c^{3/2}T_0(2b_c^3T_0^3 - 7b_ct^2T_0T_c^2 + 4t^3T_c^3)}{16t^3T_c^5(2b_cT_0 - tT_c)}(T - T_c)^2 \ldots ,$$

$$b = b_c + \frac{t(b_c - 2w)}{2(2b_cT_0 - tT_c)}(T - T_c) \tag{7.10}$$

$$- \frac{b_c^2T_0(14b_c^2T_0^2 - 21b_ctT_0T_c + 8t^2T_c^2)}{16T_c^2(2b_cT_0 - tT_c)^3}(T - T_c)^2 + \ldots ,$$

with the critical values T_c and b_c given by (3.40) and (3.43). Then

$$U_{\text{dil}} = U_0 + N^2\frac{(b_c - 2w)^2}{16w}(T - T_c)$$

$$- N^2\frac{b_c(2 + t - 5w) + 4w^2}{8(4w - t - 2)T_c}(T - T_c)^2 + \ldots , \tag{7.11}$$

where the internal energy at $T = T_c$ is

$$U_0 = -\frac{5}{12}N^2(t + 2 - 3w)T_c . \tag{7.12}$$

Note that setting $w = 1$ in (7.12) recovers (7.7), and that, again, $U_0 < 0$ in accordance with (7.2).

For the dense phase the corresponding expansions are

$$\sqrt{a} = -\frac{b_c^{3/2}T_0}{4(w - 1)tT_c^2}(T - T_c)$$

$$+ T_0b_c^{3/2}\frac{8tT_c(wT_0 - (w - 1)^2tT_c) + T_0b_c(8wT_0 + (10 - 26w + 13w^2)tT_c)}{32(w - 1)^2t^2T_c^4(2T_0b_c - tT_c)}(T - T_c)^2 \ldots ,$$

$$b = b_c + \frac{t(b_c - 2w)}{2(2b_cT_0 - tT_c)}(T - T_c) - t(b_c - 2w)$$

$$\times \frac{8(w - 1)^2t^2T_c^2 + 32w^2T_0^2 - 4w(8 - 14w + 7w^2)tT_0T_c - b_cT_0(8wT_0 + (6 - 14w + 7w^2)tT_c)}{16(w - 1)^2(2b_cT_0 - tT_c)^3T_c}$$

$$\times (T - T_c)^2 + \ldots . \tag{7.13}$$

Then

$$U_{\mathrm{den}} = U_0 + N^2 \frac{(b_c - 2w)^2}{16w} (T - T_c) - N^2 w(2 + t - 3w)T_0$$

$$\times \frac{(2 + t)(4 + 5b_c + 2t) - 4wb_c(13 + 2t) + 4w^2(b_c(18 + t) - 8(1 + t)) + 16w^3(2 - 2b_c + t)}{8t(b_c - 6w)(2 + t - 4w)(w - 1)^2 T_c^2}$$

$$\times (T - T_c)^2 \dots .$$

$$(7.14)$$

Comparing (7.11) and (7.14) we see that the first derivative of the internal energy is continuous at $T = T_c$ but there is a discontinuity in the second derivative. This corresponds to a third order phase transition.

Also, unlike the $w = 1$ case, the internal energy is an increasing function of the temperature off the critical curve $T = T_c$ for both the dilute and dense phases. In addition, it can be shown that the sign of the $(T - T_0)^2$ term in both expressions for the internal energy is negative. The phase diagram for temperatures $T \sim T_0$ is depicted in fig. 7.
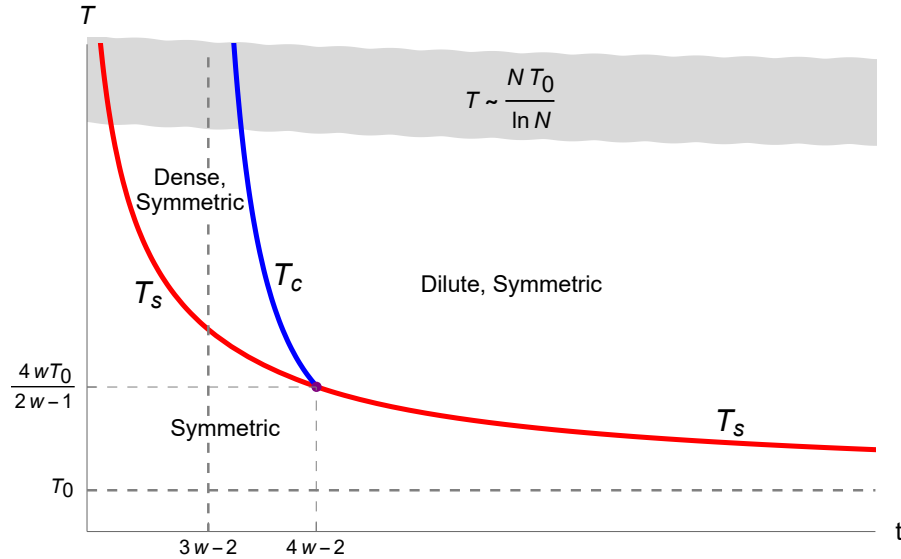

Figure 7: Phase diagram in the $t-T$ plane with a triple point intersection given by (4.18). T_s asymptotes to $T = T_0$ and $t = 0$, while T_c asymptotes to $t = 3w - 2$. The symmetric phase is everywhere stable, while the dense and dilute lumped phases are metastable for $T > T_s$ and cease to exits for $T < T_s$. For high temperatures $T \sim T_0 N / \ln N$ as indicated in the gray area, there is a nontrivial phase structure derived in section 7.2 and presented in fig. 9.

7.1.3 An alternative computation

The order of the dense-dilute transition can also be deduced from the Lagrange multiplier λ. Indeed, the discontinuity of derivatives on the (t, T) plane across the phase

boundary $T = T_c$ is the same irrespective of the direction in which we approach it. We can, thus, examine the derivative along the direction tT=constant, which amounts to keeping the parameter $x_T = tT/4T_0$ in the free energy F constant and differentiating with respect to t. Since F does not involve t explicitly, we have

$$
\left(\frac{\partial F}{\partial t}\right)_{x_T} = \int_0^\infty dx \frac{\delta F[\rho(x)]}{\delta \rho(x)} \frac{\partial \rho(x)}{\partial t}
$$

$$
\text{(using stationarity)} \quad = -N^2 T \left(\lambda \int_0^\infty dx\, x \frac{\partial \rho(x)}{\partial t} + \mu \int_0^\infty dx\, \frac{\partial \rho(x)}{\partial t} \right)
$$

$$
= -N^2 T \left(\lambda \frac{\partial}{\partial t} \int_0^\infty dx\, x\rho(x) + \mu \frac{\partial}{\partial t} \int_0^\infty dx\, \rho(x) \right)
$$

$$
\text{(using the constraints)} \quad = -\frac{N^2 T}{4}\lambda \,.
$$

(7.15)

From (3.21) in the dilute phase and (4.14) in the dense phase we see that $\lambda_{\mathrm{dil}} = \lambda_{\mathrm{den}}$ at the phase boundary $a = 0$. For $w > 1$ the first derivatives $(\partial \lambda_{\mathrm{dil}}/\partial t)_{x_T}$ and $(\partial \lambda_{\mathrm{den}}/\partial t)_{x_T}$ at $a = 0$ are also the same. This can be checked explicitly for any $w \neq 1$, but it is easily seen from the form of λ for $w = 2$ in (6.16), in which the continuity of the first derivatives arises from the fact that the step function is multiplied by a term that vanishes quadratically as $p \to q$. Using similar reasoning, the second derivatives $(\partial^2 \lambda_{\mathrm{dil}}/\partial t^2)_{x_T}$ and $(\partial^2 \lambda_{\mathrm{den}}/\partial t^2)_{x_T}$ differ at $a = 0$, leading to a discontinuity in $(\partial^3 F/\partial t^3)_{x_T}$ on the phase boundary and indicating a third-order phase transition. For $w = 1$ the absence of the first term in the expression for λ in (4.14) leads to a discontinuity already in the first derivative $(\partial \lambda/\partial t)_{x_T}$ on the phase boundary and thus to a discontinuity of $(\partial^2 F/\partial t^2)_{x_T}$, indicating a second-order phase transition.

7.2   Transitions to the disjoint phase and large temperatures

For the disjoint phase, the free energy F and energy U can be calculated from the ground state distribution (5.7) and the isolated $k_1 = N^2 y = N^2 t/4 = n$. We see that the contribution of the isolated k_1 dominates, giving a free energy macroscopically larger (of order N^3) and an entropy macroscopically smaller (of order $N \ln N$) than the

ones in the other phases, namely[6]

$$F_{\text{disj}} \simeq U_{\text{disj}} \simeq -\frac{T_0 N}{2n} n^2 = -\frac{t}{8} N^3 T_0 , \qquad S_{\text{disj}} \simeq (w-1) N \ln N . \qquad (7.16)$$

Since the free energy of the lumped phases is of order N^2, the transition at $T = T_s$ involves a jump in the free energy and is of zeroth order. This also means that, at temperatures of order T_0, the other two phases are metastable, since the disjoint phase has a macroscopically lower free energy.

The metastability frontier at which the free energy of the disjoint and either the dense or the dilute phase are equal would be at a macroscopically large temperature $T \sim T_0 N / \ln N$. As we shall see, at such temperatures a new phase appears, and the phase diagram in fig. 7 acquires extra structure.

Assume a temperature of the above order, that is,

$$T = \tau \frac{N}{\ln N} T_0 \gg T_0 , \qquad (7.17)$$

with τ a dimensionless parameter of order 1. Substituting this value in (5.4) and keeping leading-order contributions leads to

$$\lambda = \left(\frac{4y}{t\tau} - 1 \right) \ln N + \mathcal{O}(1) . \qquad (7.18)$$

We also note that the second constraint in (5.5) implies

$$0 < y \leqslant \frac{t}{4} , \qquad (7.19)$$

since the integral of $x\rho(x)$ is at least $1/2$.[7]

---

[6]These expressions follow from the exact formulae of section 2. For the fully symmetric irrep with $k_1 = n + N - 1$ and $k_i = N - i$, $i = 2, 3, \ldots, N$, (2.7) gives $\dim(\mathbf{k}) = \dfrac{(n+N-1)!}{n!(N-1)!} \sim n^N N^{-N} \sim N^N$, and (2.9) gives $d(n, \mathbf{k}) = 1$, as it should since there is only one way to compose n fundamentals into a single row. Then (2.10) yields U and the logarithm of (2.11) yields S.

[7]A proof of this statement goes as follows: From the fact that $0 < \rho(x) < 1$, we deduce that

$$x > \int_0^x dy \, \rho(y) \implies \int_0^\infty dx \, x\rho(x) > \int_0^\infty dx \, \rho(x) \int_0^x dy \, \rho(y)$$
$$= \frac{1}{2} \int_0^\infty d\left[\int_0^x dy \, \rho(y) \right]^2 = \frac{1}{2} \left[\int_0^\infty dy \, \rho(y) \right]^2 = \frac{1}{2} , \qquad (7.20)$$

where we used the first constraint in (3.5). This bound arises from the corresponding discrete sum over k_i, where the singlet representation with $k_i = 0, 1, \ldots, N-1$ clearly provides the minimum value for the sum $\sum_{i=1}^N k_i = N(N-1)/2 \simeq N^2/2$, leading to the above bound in the continuum limit.

31

The value of the Lagrange multiplier λ, and the properties of the configuration, depend on the prefactor of $\ln N$ in (7.18). Specifically:

- $\tau > 4y/t$: Then λ is large ($\sim \ln N$) and negative. This destabilizes the equation for the lumped part $\rho(x)$ and leads to no solution. Since $y \leqslant t/4$, we conclude that for $\tau > 1$ there is no solution and the disjoint phase disappears.

- $\tau < 4y/t$: Then λ is large ($\sim \ln N$) and positive. This drives the configuration for the lumped part $\rho(x)$ deep into the dense phase, that is, to (5.7), forcing y to the value $y = 1/4$. Therefore, for $\tau < 1$ the disjoint phase exists as discussed in detail in section 5.

- $\tau = 4y/t$: Then λ becomes of order 1. Therefore, the equation for the lumped part $\rho(x)$ can have a nontrivial solution. In this case,

$$\int_0^\infty dx\, x\, \rho(x) = \frac{t}{4} + \frac{1}{2} - y = \frac{t(1-\tau)}{4} + \frac{1}{2} = \frac{\tilde{t}}{4} + \frac{1}{2}, \qquad \tilde{t} = t(1-\tau). \quad (7.21)$$

Then, the equation for $\rho(x)$, becomes the standard one but with a high temperature as in (7.17) and an effective $\tilde{t} = (1-\tau)t$, with the value of λ, which is now of order 1, adjusting to the one reproducing the effective $\tilde{t}$.[8] The solution for the lumped part $\rho(x)$ is given by the large-temperature limit of the solutions found in sections 3 or 4 (depending on the value of $\tilde{t}$), and it is also calculated in [18], which examined the infinite-temperature limit of the present model. This constitutes a new phase, which exists for all $0 < \tau < 1$, consisting of a large $k_1 = N^2 \tilde{t}/4 = (1-\tau)n$ plus a nontrivial lumped part ρ.

Therefore, in the range $0 < \tau < 1$ there exist, a priori, three distinct phases: a lumped one ($y \simeq 0$), corresponding to an $SU(N)$ irrep with a distribution of row lengths of order N in its Young tableau; a disjoint-lumped one ($y = t\tau/4$), corresponding to an irrep with one long row of order $n \sim N^2$ and a distribution of lower rows of order N; and a disjoint one ($y = t/4$), corresponding to a symmetric irrep with a single row of length n. The first (lumped) phase is of paramagnetic nature, the second (mixed) one is partially ferromagnetic, and the last (symmetric) one is fully ferromagnetic.

To determine the global stability and metastability properties of the above phases we need to compare their free energy:

---

[8] The $\mathcal{O}(1)$ part of λ is not fixed by (5.4) since it can be modified by adding subleading terms in the temperature, or equivalently changing y by a subleading term.

- The free energy of the disjoint phase is already calculated in (7.16), which we reproduce here for convenience

$$F_{\text{disj}} \simeq -\frac{t}{8}N^3 T_0 \,. \tag{7.22}$$

- The free energy of the lumped phase at high temperatures $T \gg T_0$ is dominated by the entropy, that is, $F_{\text{lump}} \simeq -TS$. Further, at high temperatures the entropy approaches a limiting value S_∞ that can be obtained from the results in this paper, but is also already calculated in [18]. Dropping subleading terms in (3.86) and (3.87) of [18] we obtain, for both the dense and dilute lumped phases, $S_\infty = n \ln N = \frac{t}{4}N^2 \ln N$, which is the logarithm of the total number of states N^n of the model for all values of w. Notably, S_∞ is w-independent. Therefore, using (7.17) we obtain

$$F_{\text{lump}} \simeq -\tau \frac{t}{4}N^3 T_0 \,. \tag{7.23}$$

- The free energy of the lumped-disjoint phase can be calculated in a similar way. The end result consists of the free energy due to the entropy of the lumped part $-T\tilde{n}\ln N$, with $\tilde{n} = n(1-\tau)$, plus the energy of the isolated $k_1 = N^2 y = \tau n$, $U = -T_0 N k_1^2/(2n) = -\tau^2 t T_0 N^3/8$. Altogether,

$$F_{\text{lump-disj}} \simeq -\tau(2-\tau)\frac{t}{8}N^3 T_0 \,. \tag{7.24}$$

Comparing the three expressions in (7.22)-(7.24) we see that the lumped-disjoint phase is always metastable. In addition, the disjoint phase is globally stable and the lumped phase is metastable for $\tau < 1/2$, while their roles are reversed for $1/2 < \tau < 1$. For $\tau > 1$ only the lumped phase exists. As evident from (3.40) and fig. 7 (or from the results of [18], relevant in the present high-temperature regime), the lumped phase is in the dilute configuration for $t > 3w - 2$ and the dense one for $t < 3w - 2$.

The above picture admits a refinement. Indeed, the precise form of the disjoint phase changes slightly at $\tau = 1/(w+1)$. Comparing the free energy of the fully symmetric irrep of length n, as in footnote 6, to that of a configuration with a number of boxes $s = \mathcal{O}(1)$ in its lower rows and a top row of length $n - s$, a direct computation using the exact formulae of section 2 yields a leading order change of free energy

$$\Delta F \equiv F_{\text{sdisj}} - F_{\text{disj}} \simeq s\left(T_0 N - (w+1)T\ln N\right) = sN\left(T_0 - (w+1)\tau\right), \tag{7.25}$$

which is $\mathcal{O}(N)$, and expressed in terms of the relevant variable $\Delta x = s/N$ it is $\mathcal{O}(N^2)$, while the free energy itself is $\mathcal{O}(N^3)$. Therefore, $\Delta F \simeq 0$ to leading order in N, as expected from the fact that the disjoint is a local extremum. Nevertheless, this indicates that for

$$\tau > \frac{1}{w+1} \qquad \Longleftrightarrow \qquad T > \frac{T_0 \, N}{(w+1) \ln N} \, , \tag{7.26}$$

the fully symmetric irrep is unstable, the stable one being a "modified symmetric" configuration with a small number $s \ll n \sim N^2$ of boxes in lower rows. We call this a "pseudo-phase transition," as all thermodynamic quantities are continuous across $\tau = 1/(w+1)$ to leading order in N. For the distribution ρ, this corresponds to $\rho(x)$ deviating slightly from the step function form (5.7) near $x = 1$, developing a smooth transition from $\rho = 1$ to $\rho = 0$. The exact shape of this transition may be of mathematical interest, but it is irrelevant for the thermodynamics of the model.

Similarly, by using the results of [18], or by referring to fig. 7, if the parameter t of the model is below its large-temperature critical value, i.e. $t < 3w - 2$, then the lumped part ρ in the lumped-disjoint phase will be in the dense configuration for all τ. If, however, $t > 3w - 2$, then for $\tilde{t} < 3w - 2$ the lumped part will be in the dense phase, while for $\tilde{t} > 3w - 2$ it will be in the dilute configuration; that is,

$$
\begin{aligned}
\text{dilute-disjoint:} \quad & 0 < \tau < 1 - \frac{3w - 2}{t} \, , \\[2mm]
\text{dense-disjoint:} \quad & 1 - \frac{3w - 2}{t} < \tau < 1 \, .
\end{aligned}
\tag{7.27}
$$

Nevertheless, the two configurations have the same free energy to leading order in N as a function of τ, so they do not constitute thermodynamically distinct phases and this is another pseudo-phase transition. The free energies of all phases at large temperature as a function of τ, and for $t > 3w - 2$, are depicted in figure 8. For $t < 3w - 2$ the figure is similar, with the lumped part of the metastable mixed phase being entirely in the dense configuration (the entire curve is in deep orange and the line at $\tau = 1 - (3w - 2)/t$ missing.

The above results can be compared to those of [17], which examined the case $w = 2$ and finite N. The transition between the stable and metastable phases involved three temperatures $T_0 < T_1 < T_c$: for $T < T_0$ the ferromagnetic phase was stable and the paramagnetic one unstable; for $T_0 < T < T_1$ the paramagnetic phase became metastable; for $T_1 < T < T_c$ the ferromagnetic phase turned metastable and the para-
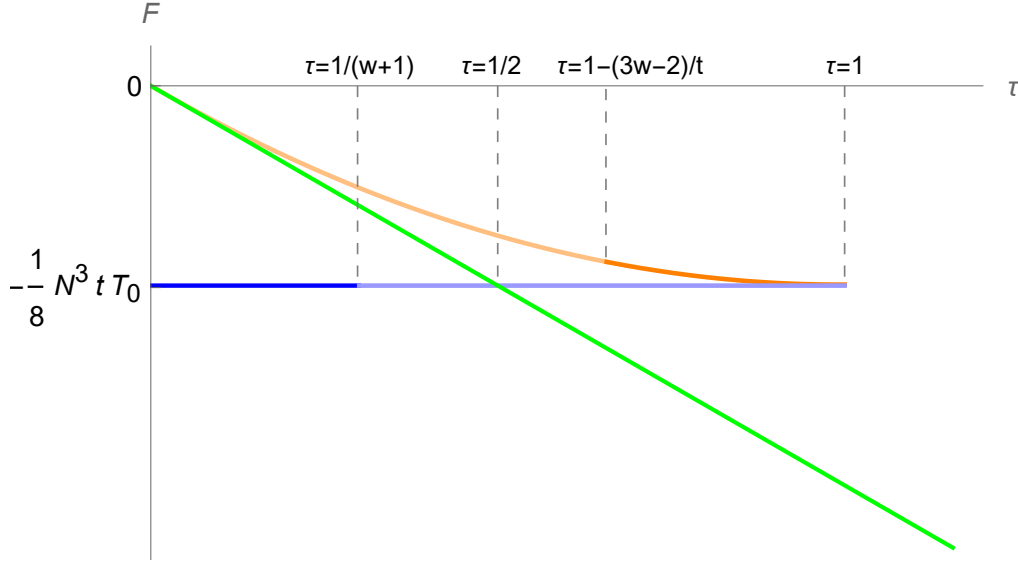
34

Figure 8: The free energy of the lumped (green), lumped-disjoint (orange), and disjoint (blue) phases as a function of the scaled temperature τ and for $t > 3w - 2$. For $\tau < 1/(w+1)$ the disjoint phase is the symmetric irrep (deep blue), while for $1/(w+1) < \tau < 1$ it has a subleading number of boxes in lower rows (light blue). Likewise, for $\tau < 1 - (3w - 2)/t$ the lumped part of the lumped-disjoint phase is in the dilute configuration (light orange), while for $1 - (3w - 2)/t < \tau < 1$ it is in the dense configuration (deep orange). We have depicted the case with $t > 2(3w - 2)$. For $3w - 2 < t < 2(3w - 2)$ the second and third dashed vertical lines are interchanged.

magnetic one became stable; and for $T > T_c$ the ferromagnetic phase ceased to exist and the paramagnetic one remained stable. For large N, the temperatures T_1 and T_c were found to behave as $T_1 \simeq T_c/2 \simeq \frac{N}{\ln N} T_0$. These precisely match the values $\tau = \frac{1}{2}$ and $\tau = 1$ in (7.17) which mark the temperatures for similar phase transitions in our case. The modified structure of these phases, however, as well as the existence of the metastable paramagnetic-ferromagnetic phase, were lost in the finite-N analysis.

The large-temperature phases on the $t-T$ plane can be depicted by trading N for the parameter t and the "volume" (number of atoms) n, and keeping n constant as we vary t and T. In this parametrization, large temperatures (7.17) become

$$T = T_L \frac{\tau}{\sqrt{t}}, \quad \text{with} \quad T_L = 4T_0 \frac{\sqrt{n}}{\ln n}, \tag{7.28}$$

where we used $\ln n \gg 1, \ln t$. Then the curve corresponding to $\tau = 1$ marks a true phase transition and the one corresponding to $\tau = \frac{1}{2}$ a metastability transition. The curves for $\tau = 1/(3w - 2)$, $t = 3w - 2$, and $\tau = 1 - (3w - 2)/t$ separate phases with qualitatively different features but thermodynamically represent pseudo-transitions, as explained earlier. The full phase diagram is presented in fig. 9.
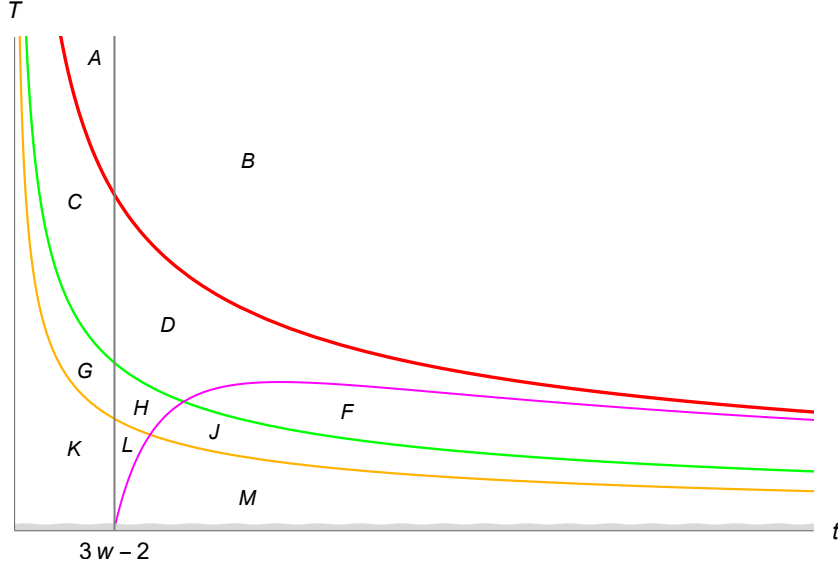
Figure 9: The phase diagram for temperatures $T \sim T_L$ at fixed number of atoms n. The upper (red) curve $T = T_L/\sqrt{t}$ marks a true phase transition and the middle (green) curve $T = T_L/2\sqrt{t}$ marks a metastability transition, while the remaining (orange, purple, gray) curves represent pseudo-transitions. The various phases are:
dense-lumped: A,C (stable) G,K (metastable); dilute-lumped: B,D,F (stable) H,J,L,M (metastable)
modified symmetric: C,D,F (metastable) G,H,J (stable); fully symmetric: K,L,M (stable)
dense-disjoint: C,D,G,H,K,L (metastable); dilute-disjoint: F,J,M (metastable)
The shaded region near the t axis represents temperatures $\sim T_0$ with phases depicted in fig. 7

8 Conclusions

The phase structure of the $SU(N)$ ferromagnet at large N manifests qualitatively new properties as compared to the finite-N case. The main novel features of the large-N model are, first, the emergence of two distinct temperature scales, and second, the appearance of additional phases and sub-phases. The two temperature scales are related by a scale factor of order $N/\ln N$, the lower one being relevant to the stability of the paramagnetic phases and the higher one to the stability of the ferromagnetic phases. The appearance of additional phases occurs both within the paramagnetic regime, which splits into two phases separated by a phase transition and leads to a triple point, and the ferromagnetic phase, which can exhibit small deviations from the fully symmetric irrep of the finite-N case, but also develops a second, thermodynamically distinct metastable phase that deviates substantially from the symmetric irrep.

The element driving the emergence of new features in the model is the Vandermonde term in the effective action (2.10, 2.11), which is thermodynamically suppressed for finite N but becomes relevant at large N. This leads to a paramagnetic phase that

36

corresponds to an irrep of $SU(N)$ other than the singlet, which changes with the temperature, and to generalized symmetry breaking patterns in the ferromagnetic phase.

Although the paramagnetic phases are metastable at low temperatures, and the novel mixed paramagnetic-ferromagnetic phase is metastable at all temperatures, their presence is physically significant. By Arrhenius' law, the transition of a metastable state to a fully stable one, when driven only by thermal fluctuations, is exponentially suppressed and the transition time is exceedingly large. For all practical purposes, metastable states are stable if left unperturbed, and only external perturbations (impurities, shaking the system etc.) can induce their decay. Our results, therefore, can be physically relevant in the appropriate context.

Potential applications of the large-N, general-w model studied in this work extend to any system where the number of degrees of freedom per atom N grows large and becomes comparable to the square root of the number of atoms $\sqrt{n}$, thus making the analysis in which the Vandermonde terms is neglected unreliable. Even for moderately high N, the large-N results may better approximate the thermodynamics of the model than the finite-N results, in cases where the two differ. Such situations can arise either when N is relatively high, or when the number of atoms n is not very high, which is the case in some experimentally prepared systems (for instance, in lattices created with trapped ions, the number of sites is of order a few tens [20]).

The model could also be relevant to more exotic situations, such as the physics of the quark-gluon plasma (for a review see, e.g., [21]), that is, a fluid of particles carrying color degrees of freedom which are assumed to ferromagnetically interact.

An obvious next step in further analyzing the large-N model would be the addition of external non-Abelian magnetic fields. Their inclusion in the finite-N model led to a highly nontrivial phase diagram in the temperature-magentic field plane, with several (meta)stable states and phase transitions appearing. In the large-N case, the thermodynamic phase space would be enlarged into the three-dimensional $T - t - B$ space, B representing the magnetic field in a single direction of $SU(N)$, potentially leading to a very rich phase structure.

In addition, several possible generalizations of our model exist, similar to the ones open in the finite-N case. A system of atoms each carrying an irrep of $SU(N)$ other than the fundamental, representing a case with reduced symmetry among the states of the atom, would be interesting to consider. Alternatively, systems involving 3-atom

or higher interactions, which would manifest in the appearance of higher Casimirs in the energy term, would be interesting to analyze in the large-N limit.

Finally, applications in matrix models and large-N Yang-Mills theories could also be envisaged (see, e.g. [22–24] and [25–28]). The possible relevance of the ferromagnetic term in the physics of microstates in two-dimensional black holes [29,30] as studied in [31,32] and more recently in [33,34], as well as in the deconfinement/Hagedorn transition in large-N gauge theories [35–39] would be an interesting and important issue. This and other related questions merit further investigation.

Acknowledgements

References

[1] M.A. Cazalilla, A.F. Ho and M. Ueda, *Ultracold gases of ytterbium: ferromagnetism and Mott states in an* $SU(6)$ *Fermi system*, 2009 New J. Phys. **11** 103033.

[2] A.V. Gorshkov *et al.*, *Two-orbital SU(N) magnetism with ultracold alkaline-earth atoms*, Nature Physics **6** (2010) 289-295.

[3] X. Zhang *et al.*, *Spectroscopic observation of* $SU(N)$*-symmetric interactions in Sr orbital magnetism*, Science Vol 345, Issue 6203 (2014) 1467.

[4] M. A. Cazalilla and A.M. Rey, *Ultracold Fermi gases with emergent* $SU(N)$ *symmetry*, 2014 Rep. Prog. Phys. **77** 124401.

[5] S. Capponi, P. Lecheminant, and K. Totsuka, *Phases of one-dimensional SU(N) cold atomic Fermi gases - From molecular Luttinger liquids to topological phases*, Ann. Phys. **367** (2016) 50-95.

[6] B. Mukherjee, J.M. Hutson and K. R. A. Hazzard, $SU(N)$ *magnetism with ultracold molecules*, 2404.15957 [cond-mat.quant-gas].

[7] H. Katsura and A. Tanaka, *Nagaoka states in the SU(n) Hubbard model*, Phys. Rev. **A87** (2013) 013617.

[8] E. Bobrow, K. Stubis and Y. Li, *Exact results on itinerant ferromagnetism and the 15-puzzle problem*, Phys. Rev. **B98** (2018) 180101(R).

[9] C. Romen and A.M. Läuchli, *Structure of spin correlations in high-temperature SU(N) quantum magnets*, Phys. Rev. Research 2 (2020) 043009.

[10] D. Yamamoto, C. Suzuki, G. Marmorini, S. Okazaki and N. Furukawa, *Quantum and Thermal Phase Transitions of the Triangular SU(3) Heisenberg Model under Magnetic Fields*, Phys. Rev. Lett. **125** (2020) 057204.

[11] K. Tamura and H. Katsura, *Ferromagnetism in d-Dimensional SU(n) Hubbard Models with Nearly Flat Bands*, Journal of Stat. Phys. volume **182**, 16 (2021).

[12] K. Totsuka, *Ferromagnetism in the SU(N) Kondo lattice model: SU(N) double exchange and supersymmetry* Phys. Rev. **A107** (2023) 033317.

[13] K. Tamura, H. Katsura, *Flat-band ferromagnetism in the SU(N) Hubbard and Kondo lattice models* arXiv:2303.15820 [cond-mat].

[14] D. Yamamoto *et al.*, *Quantum and Thermal Phase Transitions of the Triangular SU(3) Heisenberg Model under Magnetic Fields*, Phys. Rev. Lett. **125** (2020) 057204.

[15] Y. Miyazaki *et al.*, *Linear Flavor-Wave Analysis of SU(4)-Symmetric Tetramer Model with Population Imbalance*, J. Phys. Soc. Jpn. **91** (2022) 073702.

[16] H. Motegi *et al.*, *Thermal Ising transition in two-dimensional SU(3) Fermi lattice gases with population imbalance*, arXiv:2209.05919 [cond-mat].

[17] A.P. Polychronakos and K. Sfetsos, *Ferromagnetic phase transitions in SU(N)*, Nucl. Phys. **B996** (2023) 116353, arXiv:2306.01051 [hep-th].

[18] A.P. Polychronakos and K. Sfetsos, *Phase transitions in the decomposition of SU(N) representations*, Nucl. Phys. **B999** (2024), 116434, arXiv:2310.16887 [hep-th].

[19] A.P. Polychronakos and K. Sfetsos, *Composing arbitrarily many SU(N) fundamentals*, Nucl. Phys. **B994** (2023) 116314, arXiv:2305.19345 [hep-th].

[20] S. Korenblit, D. Kafri, W.C. Campbell, R. Islam, E.E. Edwards, Z.X. Gong, G.D. Lin, L.M. Duan, J. Kim, K. Kim, and C Monroe, *Quantum simulation of spin models on an arbitrary lattice with trapped ions*, New J. Phys. **14** (2012) no.9, 095024.

[21] R. Pasechnik and M. Šumbera, *Phenomenological Review on Quark–Gluon Plasma: Concepts vs. Observations*, Universe **3** (2017) no.1, 7, arXiv:1611.01533[hep-th].

[22] See, e.g., E. Martinec, *Matrix Models and 2D String Theory,* Application of random matrices in physics, NATO Advanced Study Institute, Les Houches, France, June 6-25, 2004, 403-457, hep-th/0410136.

[23] G.J. Turiaci, M. Usatyuk, and W.W. Weng, *Dilaton-gravity, deformations of the minimal string, and matrix models,*
Classical and Quantum Gravity 38 (20) 2021, arXiv:2011.06038 [hep-ph].

[24] S. Romiti and C. Urbach, *Digitizing lattice gauge theories in the magnetic basis: reducing the breaking of the fundamental commutation relations*, Eur. Phys. J. C **84** (2024) no.7, 708, [arXiv:2311.11928 [hep-lat].

[25] D.J. Gross and E. Witten, *Possible Third Order Phase Transition in the Large N Lattice Gauge Theory*, Phys. Rev. **D21** (1980), 446-453.

[26] S.R. Wadia, $N = \infty$ *Phase Transition in a Class of Exactly Soluble Model Lattice Gauge Theories*, Phys. Lett. **B93** (1980), 403-410.

[27] J.G. Russo and M. Tierz, *Multiple phases in a generalized Gross-Witten-Wadia matrix model*, JHEP **09** (2020), 081, arXiv:2007.08515 [hep-th].

[28] J.G. Russo, *Deformed Cauchy random matrix ensembles and large N phase transitions* JHEP **11** (2020), 014 arXiv:2006.00672 [hep-th] and
Phases of unitary matrix models and lattice QCD2, Phys. Rev. **D102** (2020) no.10, 105019, arXiv:2010.02950 [hep-th].

[29] E. Witten, *On string theory and black holes*, Phys. Rev. **D44** (1991), 314-324.

[30] G. Mandal, A. M. Sengupta and S. R. Wadia, *Classical solutions of two-dimensional string theory*, Mod. Phys. Lett. **A6** (1991), 1685-1692.

[31] V. Kazakov, I. K. Kostov and D. Kutasov, *A Matrix model for the two-dimensional black hole*, Nucl. Phys. **B622** (2002), 141-188, arXiv:hep-th/0101011.

[32] V. A. Kazakov and A. A. Tseytlin, *On free energy of 2-D black hole in bosonic string theory*, JHEP **06** (2001), 021, arXiv:hep-th/0104138.

[33] P. Betzios and O. Papadoulaki, *Microstates of a 2d Black Hole in string theory*, JHEP **01** (2023) 028, arXiv:2210.11484 [hep-th].

[34] A. Ahmadain, A. Frenkel, K. Ray and R. M. Soni, *Boundary Description of Microstates of the Two-Dimensional Black Hole*, SciPost Phys. **16** (2024) no.1, 020, arXiv:2210.11493 [hep-th].

[35] B. Sundborg, *The Hagedorn transition, deconfinement and $N = 4$ SYM theory*, Nucl. Phys. **B573** (2000) 349, arXiv:hep-th/9908001.

[36] O. Aharony, J. Marsano, S. Minwalla, K. Papadodimas and M. van Raamsdonk, *The Hagedorn-deconfinement phase transition in weakly coupled large N gauge theories*, Adv. Theor. Math. Phys. **8** (2004) 603-696, arXiv:hep-th/0310285.

[37] M. Hanada, J. Maltz, and L. Susskind, *Deconfinement transition as black hole formation by the condensation of QCD strings*, Phys. Rev. **D90** (2014) 105019

[38] M. Hanada, A. Jevicki, C. Peng, and N. Wintergerst, *Anatomy of deconfinement*, J. High Energ. Phys. **12** (2019) 167, arXiv:1909.09118 [hep-th].

[39] D. Berenstein and K. Yan, *The endpoint of partial deconfinement*, J. High Energ. Phys. **12** (2023) 030, arXiv:2307.06122 [hep-th].